Timescales, mechanisms, and controls of incisional avulsions in floodplain wetlands: insights from the Tshwane River, semiarid South Africa

Larkin, Zacchary T. ; Tooth, Stephen; Ralph, Timothy J.; Duller, G. A. T.; McCarthy, Terence; Keen-Zebert, Amanda K.; Humphries, Marc

Published in:
Geomorphology

DOI:
10.1016/j.geomorph.2017.01.021

Publication date:
2017

Citation for published version (APA):
Larkin, Z. T., Tooth, S., Ralph, T. J., Duller, G. A. T., McCarthy, T., Keen-Zebert, A. K., & Humphries, M. (2017). Timescales, mechanisms, and controls of incisional avulsions in floodplain wetlands: insights from the Tshwane River, semiarid South Africa. *Geomorphology*, *283*, 158-172. https://doi.org/10.1016/j.geomorph.2017.01.021

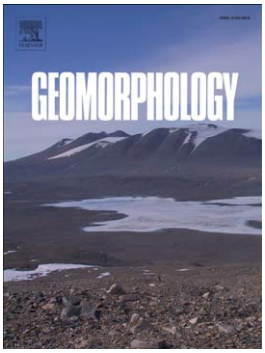

Timescales, mechanisms, and controls of incisional avulsions in floodplain wetlands: Insights from the Tshwane River, semiarid South Africa

Zacchary T. Larkin, Stephen Tooth, Timothy J. Ralph, Geoff A.T. Duller, Terence McCarthy, Amanda Keen-Zebert, Marc S. Humphries

PII: S0169-555X(16)30561-X
DOI: doi:10.1016/j.geomorph.2017.01.021
Reference: GEOMOR 5898

To appear in: *Geomorphology*

Received date: 5 July 2016
Revised date: 13 January 2017
Accepted date: 13 January 2017

Please cite this article as: Larkin, Zacchary T., Tooth, Stephen, Ralph, Timothy J., Duller, Geoff A.T., McCarthy, Terence, Keen-Zebert, Amanda, Humphries, Marc S., Timescales, mechanisms, and controls of incisional avulsions in floodplain wetlands: Insights from the Tshwane River, semiarid South Africa, *Geomorphology* (2017), doi:10.1016/j.geomorph.2017.01.021

Timescales, mechanisms, and controls of incisional avulsions in floodplain wetlands: Insights from the Tshwane River, semiarid South Africa

Zacchary T. Larkin[1]*, Stephen Tooth[2,3], Timothy J. Ralph[1], Geoff A.T. Duller[2], Terence McCarthy[3], Amanda Keen-Zebert[4], and Marc S. Humphries[5]

[1] Department of Environmental Sciences, Macquarie University, NSW, 2109, Australia

[2] Department of Geography and Earth Sciences, Aberystwyth University, Aberystwyth, SY23 3DB, UK

[3] School of Geosciences, University of the Witwatersrand, Johannesburg, Wits 2050, South Africa

[4] Division of Earth and Ecosystem Sciences, Desert Research Institute, Reno, NV 89512-1095, USA

[5] Molecular Sciences Institute, School of Chemistry, University of the Witwatersrand, Johannesburg, Wits 2050, South Africa

*Corresponding author. Email: zacchary.larkin@hdr.mq.edu.au; Tel.: +61 2 9850 6378.

Abstract

Avulsion (relocation of a river course to a new position) typically is assumed to occur more frequently in rivers with faster sedimentation rates, yet supporting field data are limited and the influence of sedimentation rate on avulsion style remains unclear. Using analysis of historical aerial photographs, optically stimulated luminescence dating of fluvial sediments, and field observations, we document three avulsions that have occurred in the last 650

years along the lower reaches of the semiarid Tshwane River in northern South Africa. Study of the modern river and abandoned reaches reveals that a downstream decrease in discharge and stream power leads to reduced channel size and declining sediment transport capacity. Bank erosion drives an increase in channel sinuosity, leading to a decline in local channel slope, and to a further decrease in discharge and sediment transport. Local sedimentation rates >10 mm a^{-1} occur within and adjacent to the channel, so over time levees and an alluvial ridge develop. The resulting increase in cross-floodplain gradient primes a reach for avulsion by promoting erosion of a new channel on the floodplain, which enlarges and extends by knickpoint retreat during periods of overbank flow. Ultimately, the new channel diverts the discharge and bedload sediment from the older, topographically higher channel, which is then abandoned. Our findings support the assumption that avulsion frequency and sedimentation rate are positively correlated, and we demonstrate that incisional avulsions can occur in settings with relatively rapid net vertical aggradation. The late Holocene avulsions on the semiarid Tshwane River have been driven by intrinsic (autogenic) processes during meander belt development, but comparison with the avulsion chronology along a river in subhumid South Africa highlights the need for additional investigations into the influence of hydroclimatic setting on the propensity for avulsion.

Keywords: geochronology; channel change; sedimentation rate; drylands

1. Introduction

Avulsion is the shift of a river course to a new position on a floodplain or delta and is a key process by which many rivers form new channels and adjust laterally (Smith et al., 1989; Slingerland and Smith, 2004; Stouthamer and Berendsen, 2007; Phillips, 2011). Following avulsion, the original channel may be abandoned or it may continue to operate alongside

the new channel as a distributary or anabranch. Avulsions have significant implications for the lateral redistribution of water, sediment, and nutrients and thus are a key influence on floodplain and delta geomorphology, sedimentology, and ecology (Makaske et al., 2002, 2012; Slingerland and Smith, 2004; Tooth et al., 2007; Phillips, 2012; Ralph et al., 2016). Avulsions also affect human land use and settlement in these environments, as shown by various archaeological investigations in Holocene palaeoenvironments (e.g., Morozova, 2005; Macklin and Lewin, 2015).

Despite the importance of avulsion along many rivers, the controls on the frequency and style of avulsion remain unclear. Avulsion frequency and vertical sedimentation rate are commonly assumed to be positively correlated so that avulsions occur only infrequently on slowly aggrading rivers but more frequently on rapidly aggrading rivers (Bridge and Leeder, 1979; Bryant et al., 1995; Mackey and Bridge, 1995; Schumm et al., 1996; Slingerland and Smith, 1998; Jerolmack and Mohrig, 2007; Stouthamer and Berendsen, 2007; Hajek and Wolinsky, 2012; Hajek and Edmonds, 2014). This reflects the fact that most sedimentation occurs within or near the channel, forming levees and/or alluvial ridges. These topographic features increase cross-floodplain gradient, promoting overbank flow away from the channel and providing a slope advantage for new channels forming through floodplain scour (Brizga and Finlayson, 1990; Jones and Schumm, 1999). While an assumption of a positive correlation between avulsion frequency and vertical sedimentation rate is thus physically reasonable, well-constrained field data remains lacking to quantify the relationship more precisely over Holocene and longer timescales (Tooth et al., 2007; Phillips, 2009, 2012; Donselaar et al., 2013).

The relationships between avulsion style and sedimentation rate are less clear. Nevertheless, at least two of the three main avulsion styles, defined by Slingerland and Smith (2004) as progradational, incisional, and reoccupational (also termed 'avulsion by annexation') are commonly associated with different sedimentation rates (Table 1).

Table 1

Summary of the three main avulsion styles (after Slingerland and Smith, 2004)

Avulsion style	Process of new channel formation	Relationship with sedimentation rate	Examples	References
Progradational	Overbank flows form large crevasse splays, in which a channel network develops and extends downstream, eventually forming a new channel	Most commonly associated with relatively rapid vertical sedimentation rates (>1 mm^{-1})	Cumberland Marshes and upper Columbia River, Canada Rhine-Meuse Delta, Netherlands Baghmati River, India Pantanal, Brazil	Smith et al., 1989; Morozova and Smith, 2000; Stouthamer and Berendsen, 2000, 2001; Makaske et al., 2002, 2012; Jain and Sinha, 2004; Assine, 2005;
Incisional	Overbank flows returning to a channel erode a knickpoint that retreats upstream forming a new channel once it reconnects with the original channel	Most commonly associated with relatively slow vertical sedimentation rates (<1 mm^{-1})	Cooper Creek, Australia Klip River, South Africa	Knighton and Nanson, 1993; Gibling et al., 1998; Tooth et al., 2007
Reoccupational	Reoccupation and reworking of an abandoned channel on the floodplain	Associated with slow and rapid vertical sedimentation rates	Lower Mississippi River, Nueces River, and Trinity River, USA	Aslan and Blum, 1999; Aslan et al., 2005; Phillips, 2009

Irrespective of the frequency and style of avulsion, previous studies have shown that for avulsion to occur the river must be near an avulsion threshold and that the final trigger is typically a large flood or closely spaced series of floods (Jones and Schumm, 1999). A variety of local physiographic and climatic factors can influence the timing and patterns of flooding, as well as the locations of newly avulsing channels. These include decreases in floodplain

confinement (Tooth, 1999, 2005), ice jams (Smith and Pearce, 2002), vegetation encroachment or debris blockages such as log jams (Ralph and Hesse, 2010; Phillips, 2012), beaver dams (Polvi and Wohl, 2013), hippopotami trails (McCarthy et al., 1992; Ellery et al., 2003; Tooth et al., 2007), and substrate composition (Aslan et al., 2005).

Most previous studies of avulsion have focused on humid rivers in tropical or temperate regions and, despite some notable exceptions (Smith et al., 1997; Judd et al., 2007; Tooth et al., 2007; Donselaar et al., 2013; Li et al., 2014; Li and Bristow, 2015), fewer studies of avulsion have focused on dryland rivers. In particular, while some dryland rivers are associated with extensive floodplain wetlands that in part owe their formation to avulsive redistributions of water and sediment, well-constrained field data necessary to define the relationships between sedimentation rate, avulsion frequency, and avulsion style remain limited (Tooth et al., 2007). To clarify these relationships, this study develops a chronology of floodplain sedimentation and avulsion for the lower reaches of the Tshwane River, located in the upper Limpopo River catchment in semiarid, northern South Africa (Fig. 1A). The aims of this study are to (i) combine analysis of aerial photography with optically stimulated luminescence (OSL) dating to determine the spatial pattern and chronology of avulsions; (ii) assess whether avulsion frequency and sedimentation rates are positively correlated; (iii) evaluate the influence of sedimentation rates on avulsion style; and (iv) discuss the relative importance of intrinsic (e.g., flow-sediment dynamics) and extrinsic (e.g., hydroclimatic) factors in controlling avulsion.

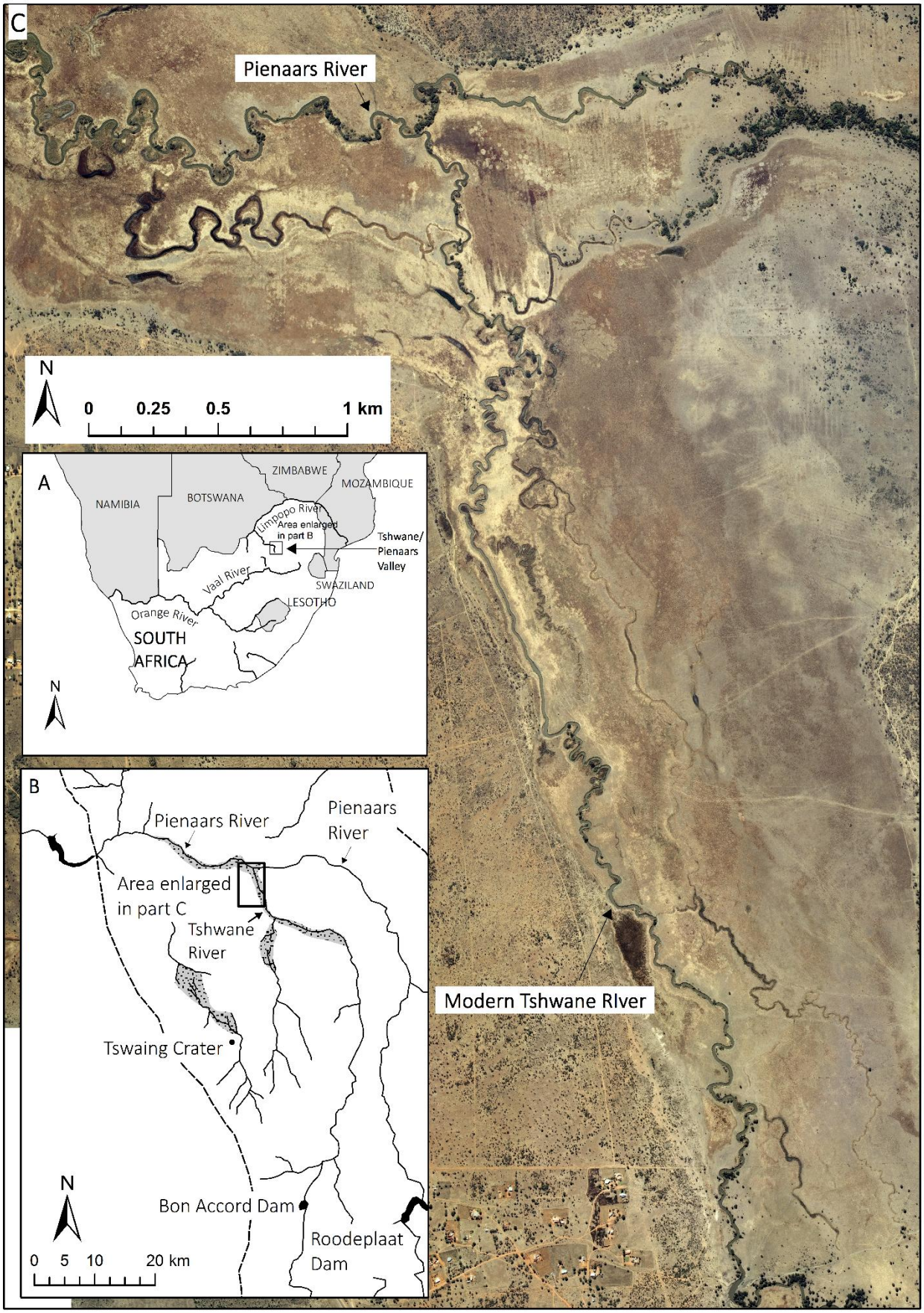

Fig. 1. The Tshwane catchment and study site: (A) location within northern South Africa; (B) the Tshwane River and part of the Pienaars River, showing the location of the study site near the confluence; (C) aerial photograph (2012) illustrating the modern channels and numerous palaeochannels near the Tshwane-Pienaars confluence (source: National Geo-spatial Information, Department of Rural Development and Land Reform, Mowbray, South Africa).

2. Regional setting

The geology of the upper Tshwane River catchment comprises mainly Pretoria Group shales and quartzites and Bushveld Complex granites. The middle and lower catchment comprises mainly sandstones, mudstones, and shales of the Karoo Supergroup (Ecca and Irrigasie formations) but outcrop is limited. The Tshwane headwaters arise in the Magaliesberg at ~1470 masl, and the river flows north toward the Pienaars River (Fig. 1B). Slope, discharge, and stream power decrease downstream; and the channel becomes less confined, smaller, and more sinuous as it traverses extensive (1-2 km wide) floodplain wetlands (Larkin et al., in press; see Table A.1). In the lower reaches, the Tshwane River is characterised by a prominently leveed, single-thread, meandering channel of variable sinuosity and is flanked by numerous oxbows, palaeochannels 1-5 km long, and backswamps (Figs. 1C and 2A). Near the diffuse confluence with the Tshwane, the Pienaars River displays similar characteristics (Fig. 1C). The Tshwane-Pienaars floodplain wetlands remain in a near-natural condition, with human influences restricted to some subsistence grazing on the floodplain. Collectively, the floodplain wetlands cover ~55 km^2, and their geomorphology indicates that river avulsion has been a key process in their development. Other than the study by Larkin et al. (in press), the rivers and floodplain wetlands have not been subject to previous detailed investigations, with avulsion chronologies remaining unknown.

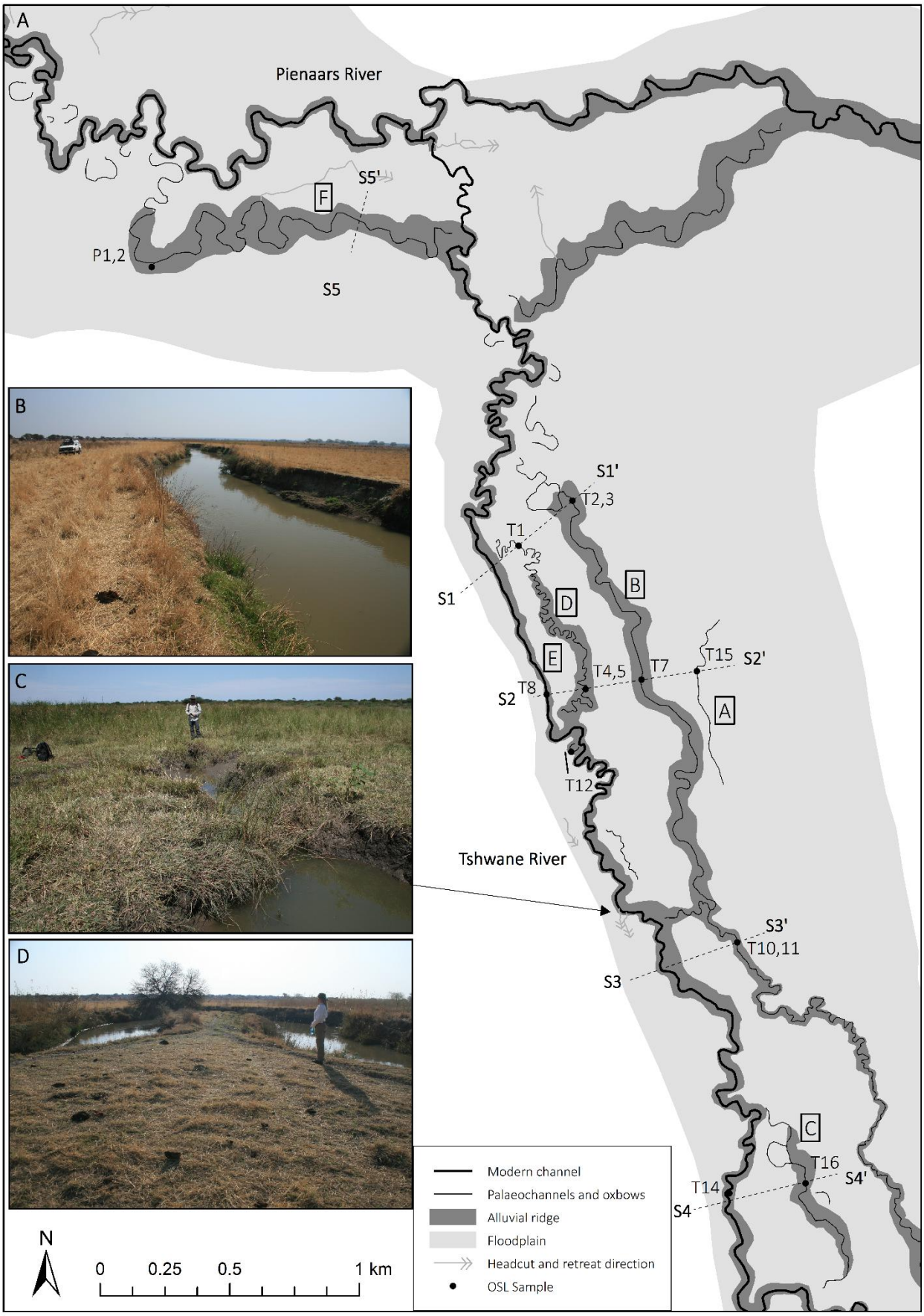

Fig. 2. (A) Geomorphological map of the Tshwane-Pienaars floodplain wetlands showing the location of the 13 OSL samples along four surveyed transects (S1-S4), and the locations of a further two samples (P1, 2) that were taken from an abandoned alluvial ridge on the Pienaars River floodplain (near transect S5). Letters A to F refer to discrete sections of the modern channel or the palaeochannels (see text). Flow direction is from south to north in the Tshwane River and from east to west in the Pienaars River. Photographs illustrating key geomorphological features at the study site: (B) relatively straight reach of the Tshwane River (view looking NNW, with flow away from the camera); (C) current headcut (~1 m tall) that has extended headward for some tens of metres from the channel bank toward a reedbed in an adjacent backswamp (view looking SSW, with flow toward the camera; arrow indicates location in study reach); (D) tight meander bend on a sinuous reach of the Tshwane River (looking WSW, with flow from left to right).

Rainfall in the study area is strongly seasonal with distinct wet (November through March) and dry (April through October) seasons. Mean annual precipitation in the Tshwane catchment is ~585 mm, falling mostly during convective thunderstorms; while mean annual potential evaporation is ~1750 mm (Working for Wetlands, 2008; Gauteng Department of Agricultural and Rural Development, 2011). Flow in the Tshwane River is perennial but strongly seasonal, with high wet season flows (>60 $m^3 s^{-1}$) and low dry season flows (<4 $m^3 s^{-1}$; Department of Water Affairs Hydrological Services, 2015). During the wet season, the Tshwane River floodplain is inundated regularly; but during the dry season, low flows are confined to the main channel, while oxbows, palaeochannels, and backswamps gradually desiccate. The lower Tshwane River transports a mixed load of slightly gravelly sand, silt, and clay, but there are no sediment transport measurements. The floodplain surface is comprised mainly of clay, with sandier sediment restricted to active channel beds and levees. Palaeochannels have been infilled to varying degrees by clastic and organic sediment but typically are preserved as <1.5-m-deep depressions with minor levees.

3. Methods

Historical aerial photograph analysis and OSL dating was used to determine the spatial pattern and chronology of avulsions. Aerial photographs at 1:32, 000 and 1:36, 000 scale from 1950, 1972, 2005, and 2012 were used to produce geomorphological maps and a time series of channel change along the lower Tshwane River. From the geomorphological maps, four distinct palaeochannel belts (labelled A-D) were selected for detailed investigation (Fig. 2A). A reach of the modern Tshwane (labelled E) and a prominent palaeochannel belt (labelled F) of the Pienaars River (Fig. 2A) were also investigated. Detailed topographic surveys of the channel, floodplain, and palaeochannel belts were undertaken using an automatic level along five transects (Fig. 2A).

3.1. Field sampling

Eleven palaeochannel samples, one oxbow sample, and three levee/alluvial ridge samples were collected for OSL dating (Fig. 2A). Palaeochannel samples (T1-T5, T7, T10, T11, T15, T16) were collected by hand augering through the organic and clay-rich infills until medium-coarse sand was encountered (sediment terminology follows the Udden-Wentworth scale; Wentworth, 1922). Following the approach adopted in previous similar studies (Rodnight et al., 2005, 2006), a ~30-cm-long, ~7-cm-diameter metal tube was then attached to the end of the auger extension rods. The metal tube was pushed into the sand at the base of the auger hole, and the sample retrieved without exposure to sunlight. One oxbow sample (T12) was collected by digging through ~45 cm of organic-rich infill with a spade, and a metal tube was then hammered horizontally into the underlying sand. These sand samples are representative of the last time that the palaeochannels and oxbow were actively transporting bedload. Sample T8 was collected from levee deposits along the modern

channel by hammering a steel tube horizontally into an eroded bank exposure and is representative of the start of overbank sedimentation at this location. Samples P1 and P2 were collected from the alluvial ridge of the abandoned Pienaars River palaeochannel using a percussion coring system that was capable of extracting intact 1-m sections of sediment to a depth of >5 m. These samples are representative of overbank sedimentation on this part of the Pienaars floodplain. All OSL sample tubes and percussion cores were extracted without exposing the sediment to sunlight and then wrapped in light-tight black plastic for transport to the laboratory, where subsequent sample treatment took place in subdued red-light conditions.

3.2. Laboratory methods

The OSL samples were processed in the Aberystwyth Luminescence Research Laboratory at Aberystwyth University. Standard methods were used to isolate the 125-212 µm quartz fraction of sediment, to dissolve carbonates and organics (hydrochloric acid and hydrogen peroxide, respectively), to remove heavy minerals and feldspars by density mineral separations, and to etch grains with 40% hydrofluoric acid in order to remove the α-irradiated outer grain surface (see Aitken, 1998).

Luminescence measurements were made on a Risø automated TL/OSL reader equipped with a single-grain system based on a 532-nm green laser (Bøtter-Jensen et al., 2003). Luminescence emitted by grains was detected with an EMI 9235QA photomultiplier, with the light filtered through 2.5 mm of U-340 to reject the stimulation source. Prior to single-grain OSL analysis, a dose recovery and preheat test was performed to determine the optimum thermal treatment for the samples to be used in the single aliquot regenerative dose (SAR) procedure (Wintle and Murray, 2006). All samples were measured with a

preheat temperature of 220°C for 10 seconds and a cut-heat of 160°C for 10 seconds. At least 800 grains were analysed for each sample, and individual grains were accepted based on criteria outlined in Jacobs et al. (2006), which are: recycling ratio within 10% of unity; test dose error <10%; T_n signal greater than three times the standard deviation of the background; and an IR-OSL depletion ratio within 10% of unity (Duller, 2003). After application of these criteria, between 135 and 495 individual equivalent dose (D_e) values were determined using Analyst software (Duller, 2015). All samples display D_e distributions that indicate heterogeneous bleaching prior to burial (see Fig. A.1 for radial plots) and are relatively young (<1 ka). Therefore, the unlogged minimum age model was used to calculate D_e values for each sample (Galbraith et al., 1999) as implemented in the R package 'Luminescence' (Fuchs et al., 2015).

The environmental dose rate was calculated by thick source α counting and β counting of dried and milled material taken from the ends of sample tubes, as this is representative of sediment surrounding the OSL sample. The cosmic ray contribution was estimated from the data given by Prescott and Hutton (1994), taking into account altitude, geomagnetic latitude, and thickness of sediment overburden. Water content was measured and kept constant for palaeochannel and oxbow samples at 25 ± 5% and at 15 ± 5% for levee samples, which dry out more readily and regularly than samples in the base of infilling channels. Equivalent dose is divided by the dose rate to derive an OSL age estimate (Duller, 2004).

4. Results

Aerial imagery, geomorphological mapping, OSL dating, and field observations provide insight into the timing and mechanisms of avulsion on the lower Tshwane River. Historical

channel changes and OSL analytical data and ages are presented in Figs. 3-6 and Tables 2 and 3.

4.1. Historical channel change in the Tshwane floodplain wetlands

Although the low resolution aerial imagery (scale 1:32, 000 to 1:36, 000) precludes accurate calculation of channel lateral migration rates, 14 meander bend cutoffs can be identified in the ~4-km-long study reach over the 62 years from 1950 to 2012. In addition, between 1950 and 1972, an avulsion led to abandonment of a highly sinuous (~2.7) reach of the main channel (palaeochannel belt D) and formation of a new, straighter channel reach (channel E) (Figs. 2B, 3A-B, 4A). Based on observations of current headcuts in this reach (Figs. 2C and 3D), this avulsion appears to have taken place as a result of headcut retreat through a backswamp that prior to 1950 existed on the western floodplain margin. Once the headcut joined the main channel upstream, the backswamp desiccated and the original channel appears to have been abandoned very quickly, with loss of definition resulting from partial infilling at its upstream and downstream ends already evident on the 1972 aerial imagery (Fig. 3B).

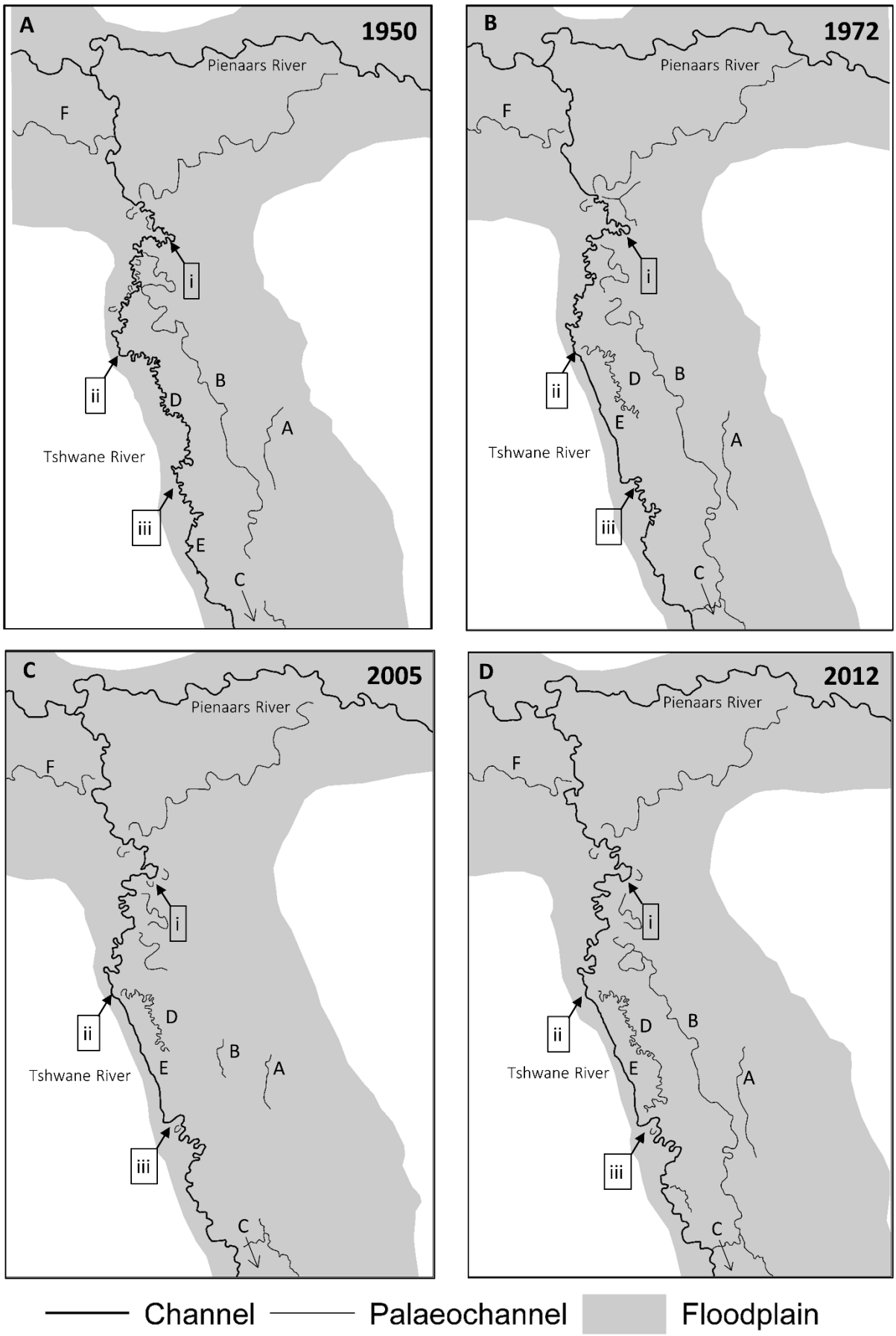
A
1950
Pienaars River
F
i
ii
B
D
A
Tshwane River
iii
E
C
B
1972
Pienaars River
F
i
ii
D
B
E
A
Tshwane River
iii
C
C
2005
Pienaars River
F
i
ii
D
B
E
A
Tshwane River
iii
C
D
2012
Pienaars River
F
i
ii
D
B
E
A
Tshwane River
iii
C
Channel
Palaeochannel
Floodplain

Fig. 3. Time series maps of the Tshwane-Pienaars floodplain wetlands derived from aerial photography: (A) 1950, (B) 1972, (C) 2005, and (D) 2012. Flow direction is from south to north in the Tshwane River and from east to west in the Pienaars River. Channel and palaeochannel belts are labelled A to F. Palaeochannels are not clearly visible in all aerial photographs owing to tonal contrast and changing vegetation and water levels. Black arrows (numbered i to iii) are shown in the same location of each frame to highlight some of the more easily visible adjustments of the river (meander cutoff or avulsion) between 1950 and 2012.

This recent avulsion led to a net shortening of the Tshwane River's length by ~1 km and thus resulted in local channel steepening. The gradient of the new channel is roughly the same as the local floodplain gradient (~0.0009 m m^{-1}) owing to its relative straightness and alignment with the valley orientation, although field observations reveal evidence of ongoing bank erosion that is leading to a slight increase in sinuosity (Fig. 2B). By contrast, upstream and downstream of the avulsion reach, more noticeable net increases in sinuosity have occurred over the historical period from ~1.31 to 1.90 and ~1.25 to 1.61, respectively (Figs. 4A-B). These sinuosity increases indicate rapid channel lateral migration (i.e., the extension and translation of meander bends; Fig. 2D) that have more than compensated for the reduction in channel length associated with the 14 meander cutoffs in the study reach during the same period.

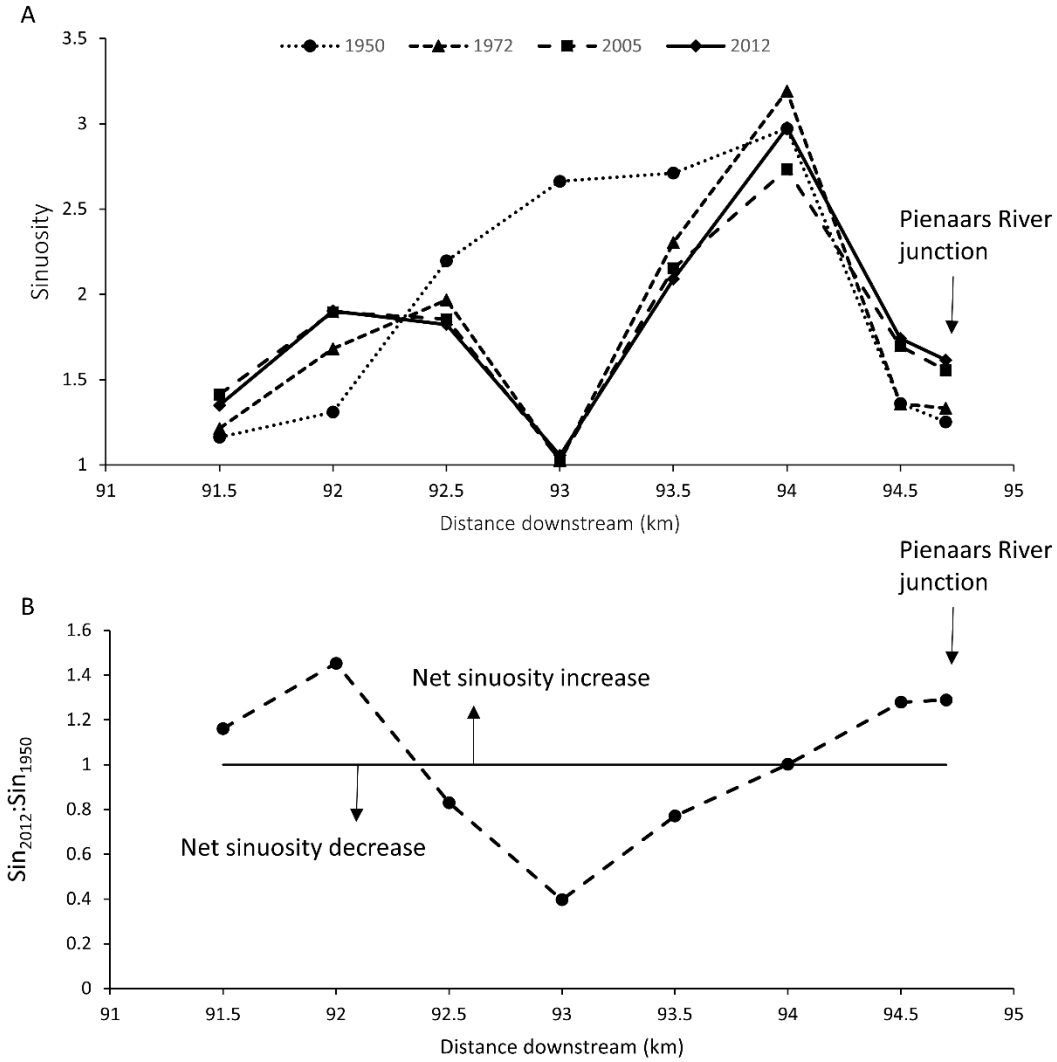

Fig. 4. (A) Sinuosity variations along 500-m reaches of the lower Tshwane River between 1950 and 2012. Distance downstream is the floodplain distance, as measured from the river's source. Note the profound influence of the 1950-1972 avulsion on sinuosity in subsequent years. (B) $Sinuosity_{2012}$:$Sinuosity_{1950}$ ratio illustrates reaches with net increases or decreases in sinuosity between 1950 and 2012.

4.2. Late Holocene chronology of avulsion and sedimentation rates

The accuracy of the OSL ages (Table 2) can be tested at some locations by comparing them with historical channel changes reconstructed from the aerial photographs. For example, sample T12 (see location in Fig. 2A) is from sediment in an oxbow that was cut off between

1972 and 2005 (point iii in Figs. 3B - 3C), and the OSL age is 40 ± 5 years (ca. A.D. 1975). Sample T8 (Fig. 2A) is from the base of the levee along the channel reach that formed during the period 1950-1972 (Figs. 3A-B), and the OSL age is 55 ± 5 years (ca. A.D. 1960). Sample T14 (Fig. 2A) is from sediment at shallow depth on a modern point bar. Comparative aerial photographs for the wider reach show that the bend has not changed significantly in recent decades, and the OSL age is 25 ± 10 years (c. AD 1990). The accuracy of the OSL ages is further demonstrated by the fact that (i) the ages for samples that were collected in vertical sequences are in the correct stratigraphic order; and (ii) the ages for samples collected from similar stratigraphic positions but at different locations along the same palaeochannel are very similar (e.g., samples T1 and T5, and samples T3, T7, and T11; Fig. 5).

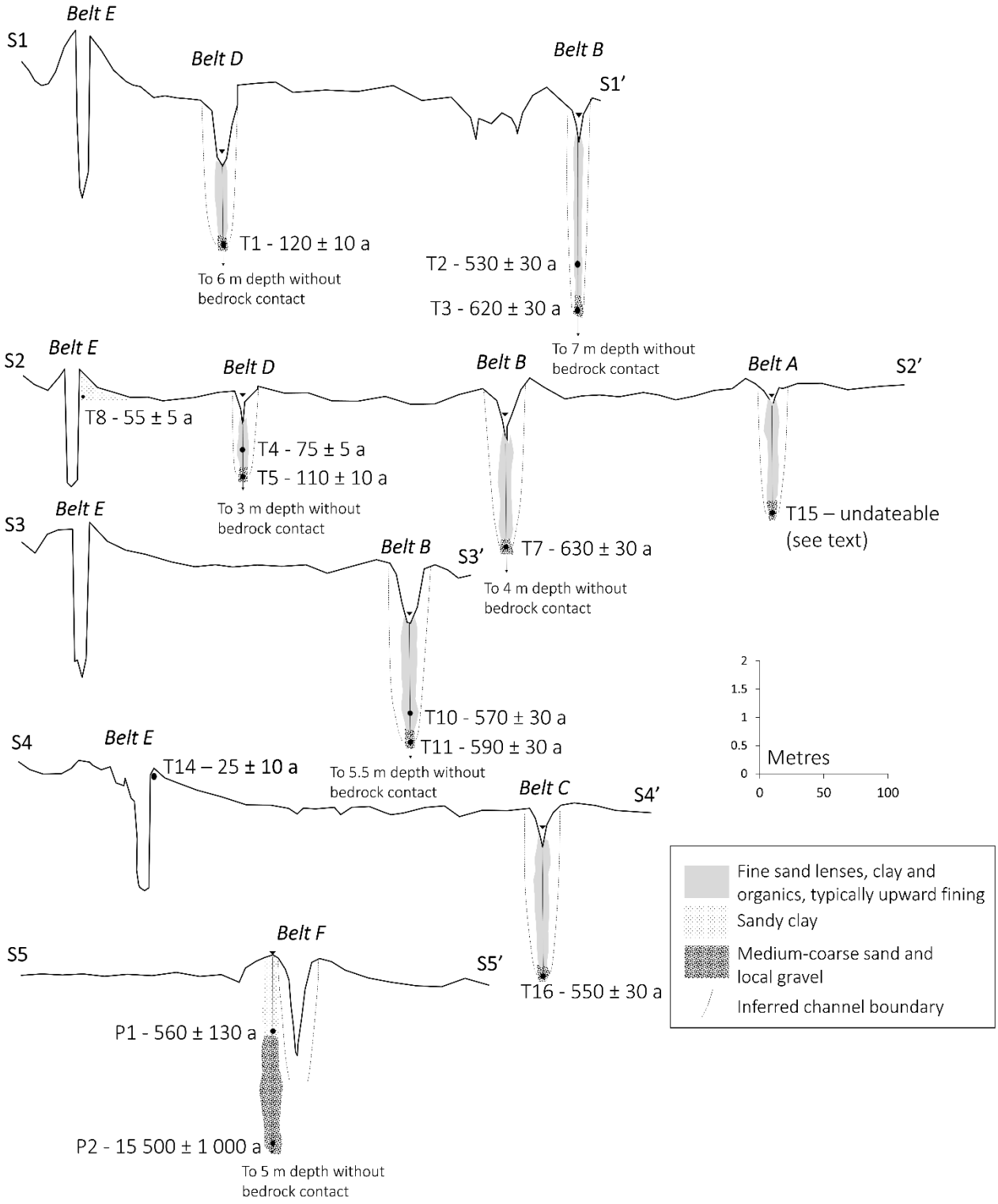

Fig. 5. Cross-sectional surveys S1-5 (see Fig. 2A for location), showing sedimentology and OSL sample codes and ages. Sample T15 in palaeochannel belt A could not be dated owing to an unusual equivalent dose distribution (see text and Fig. A.1) but, on geomorphological grounds, is likely older than the other palaeochannels. Note that the core taken from the Pienaars alluvial ridge was taken downvalley of transect S5 (Fig. 2A) but for diagrammatic purposes has been shown in an equivalent position on the survey. In the

palaeochannels, a relatively sharp boundary exists between sandy bedload sediment and the overlying finer-grained infill. The thickness of alluvium in the Tshwane-Pienaars floodplain wetlands is unknown but based on the results from augering of palaeochannel B appears to exceed 7 m.

The OSL ages reveal that the dated palaeochannels on the lower Tshwane and Pienaars floodplain are all late Holocene in age (Table 2; Fig. 5). Those ages determined from medium-coarse sand in palaeochannels and oxbows are interpreted as representing the age of some of the last significant bedload transport events and therefore provide a maximum age for abandonment of the reach or bend. Palaeochannel belt B was actively transporting medium-coarse sand bedload until ~590 years ago, palaeochannel belt C until ~550 years ago, and palaeochannel belt D until ~110 years ago. Although we collected a sample from palaeochannel belt A (T15), the D_e distribution is highly unusual (see Fig. A.1) and could not be used to provide a minimum D_e estimate using the minimum age model. As such this sample was omitted from subsequent analyses, although given its easternmost location this is likely to be one of the oldest palaeochannel belts on the lower Tshwane floodplain.

Table 2

OSL sample details and single grain analytical results

(Palaeo)channel belt	Sample[b]	Sample type	Depth (m)	N[c]	OD (%)[d]	Equivalent dose (MAM; Gy)	Dose rate (Gy ka $^{-1}$)	Age (a)
A	T15	Palaeochannel	1.81 ± 0.10	495	68	-	1.76 ± 0.08	-
B	T2	Palaeochannel	1.60 ± 0.10	202	65	0.98 ± 0.09	1.86 ± 0.09	530 ± 30
	T3	Palaeochannel	2.15 ± 0.10	341	96	1.08 ± 0.01	1.74 ± 0.08	620 ± 30
	T7	Palaeochannel	1.68 ± 0.10	252	45	0.97 ± 0.01	1.54 ± 0.08	630 ± 30
	T10	Palaeochannel	1.48 ± 0.08	378	49	1.18 ± 0.01	2.07 ± 0.10	570 ± 30
	T11	Palaeochannel	1.95 ± 0.10	219	40	1.03 ± 0.01	1.76 ± 0.08	590 ± 30
C	T16	Palaeochannel	2.10 ± 0.10	272	90	0.84 ± 0.01	1.54 ± 0.07	550 ± 30
D	T1	Palaeochannel	1.05 ± 0.10	188	100	0.23 ± 0.01	1.96 ± 0.10	120 ± 10
	T4	Palaeochannel	0.38 ± 0.08	135	25	0.14 ± 0.01	1.81 ± 0.08	75 ± 5
	T5	Palaeochannel	0.85 ± 0.05	134	71	0.20 ± 0.01	1.91 ± 0.09	110 ± 10
E (modern)	T8	Levee	0.55 ± 0.05	136	41	0.12 ± 0.01	2.27 ± 0.11	55 ± 5
	T12	Oxbow	0.53 ± 0.08	167	100	0.06 ± 0.01	1.47 ± 0.06	40 ± 5
	T14	Point bar	0.00 ± 0.05	184	100	0.03 ± 0.01	1.16 ± 0.05	25 ± 10
F	P1	Abandoned alluvial ridge	1.13 ± 0.13	199	92	1.17 ± 0.27	2.10 ± 0.11	560 ± 140
	P2	Alluvial ridge substrate	2.88 ± 0.13	299	55	30.4 ± 1.44	1.97 ± 0.09	15 500 ± 1100

Notes:

[a] Ages are rounded to the nearest 10 years if 100-1000 years old, and to the nearest 5 years if <100 years old. Ages are given in years before the measurement date of A.D. 2015. An age could not be determined for the sample from palaeochannel belt A (see text). See Fig. 2A for sample locations, Fig. A.1 for radial plots, and Table A.2 for dosimetry data.

[b] The full code for samples is Aber219/TSW or Aber219/PC; but for illustrative purposes and brevity, codes have been simplified to a prefix 'T' or 'P'.

[c] Number of grains giving a D_e.

[d] Overdispersion parameter (OD).

The medium-coarse sand in the base of the palaeochannels is overlain by fine sand lenses, clay, and organics. The fine sand lenses are interpreted as representing bedload transport during the waning phases of channel activity. Based on the OSL ages collected in vertical sequence (Fig. 5), infill sedimentation rates during these waning phases can be calculated

for two sites along palaeochannel belt B and one site along palaeochannel belt D. These infill rates vary from 6.1 to 23.5 mm a^{-1} (Table 3; Fig. 6). In addition, by assuming an age of zero years for each of the clay-rich palaeochannel fill surfaces, linear regressions for the age-depth profiles can be used to determine the time-averaged sedimentation rates over the waning and post-abandonment phases. These infill sedimentation rates vary between ~3.0 and ~7.4 mm a^{-1} over the past ~600 years (Figs. 6A-C). The levee sedimentation rate over the past ~60 years along the newly formed channel (belt E) is ~11.5 mm a^{-1} (Table 3). The OSL ages for sediment associated with palaeochannel belt F indicate that long-term (>1 ka) sedimentation rates along this particular alluvial ridge of the Pienaars River may have been lower than the shorter-term rates for infilling palaeochannels or levee sedimentation along the lower Tshwane River. Based on the two OSL ages and an assumed surface age of zero years, the average sedimentation rate alongside palaeochannel F over the last ~15 ka has been ~0.2 mm a^{-1} (Table 3; Fig. 6D), although this is likely to be a minimum estimate (see Table 3 footnote).

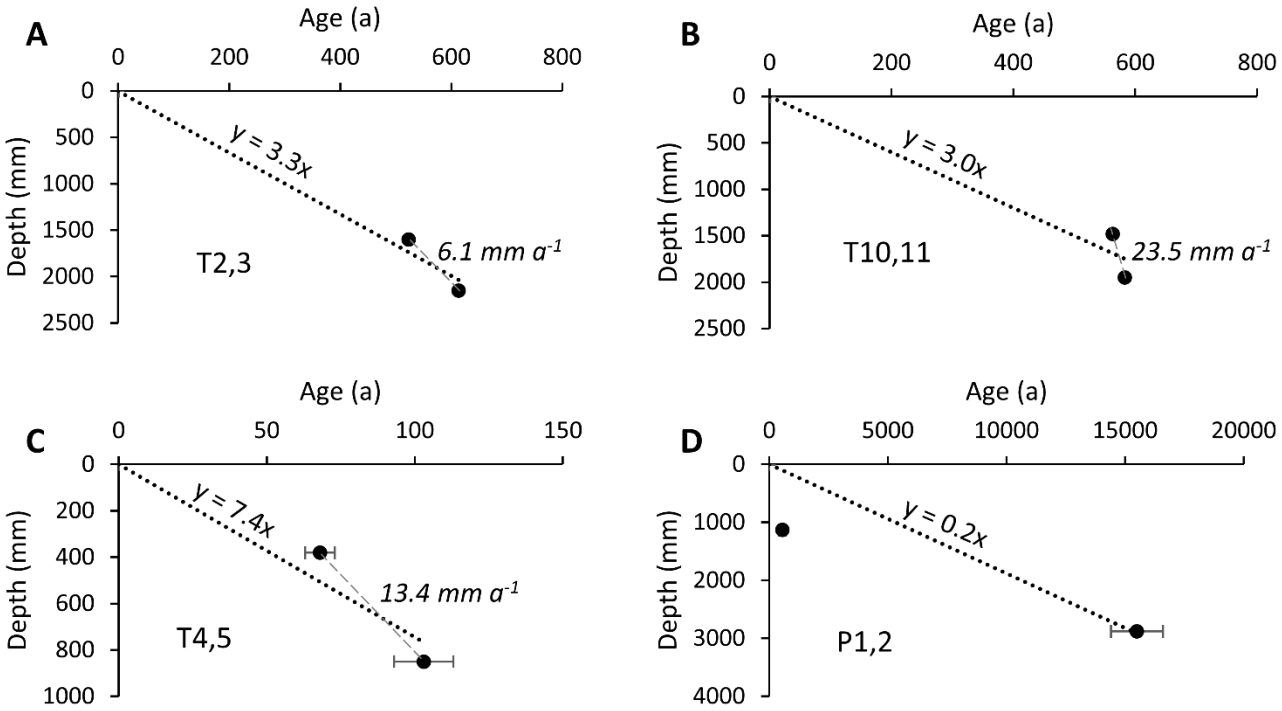

Fig. 6. Age-depth profiles for the four coring sites with OSL samples in vertical sequence: (A) and (B) palaeochannel belt B; (C) palaeochannel belt D; and (D) palaeochannel belt F. The slope of the regression line fitted through time and depth zero, given by the equation, equals the mean sedimentation rate in mm a^{-1}. Italicised sedimentation rates on A-C represent sedimentation rates between the two ages in the profile that we interpret as indicative of sedimentation rates during waning fluvial activity along the reach. Ages for the 'T' samples have been adjusted to their age at collection in 2008. Error bars are included on the ages but are too small to discern on some samples.

Table 3

Sedimentation rates and floodplain gradients for each (palaeo)channel belt

(Palaeo) channel belt	OSL sample	Depth (mm)	Age (a) [b]	Sedimentation rate (mm a^{-1}) [c]			Mean levee height (m) [d]	Floodplain gradient		
				Infill	Infill (waning flows)	Levee/ alluvial ridge		Down-stream (D/S)	Cross-floodplain (XFP)	D/S:XFP[e]
A	T15	1810	-	-	-	-	0.22	0.001	0.0049	0.20
B	T2	1600	530	3.3[f]	6.1[g]	-	0.29	0.001	0.0073	0.13
	T3	2150	620			-				
	T7	1680	630	2.7	-	-				
	T10	1480	570	3.0[f]	23.5[g]	-				
	T11	1950	590			-				
C	T16	2100	550	3.8	-	-	0.16	0.001	0.0029	0.34
D	T1	1050	120	9.3	-	-	0.22	0.001	0.0034	0.29
	T4	380	75	7.4[f]	13.4[g]	-				
	T5	850	110			-				

E (modern)	T8	550	55	-	-	11.5	0.41	0.001	0.011	0.09
	T12	530	40	-	-	-				
	T14	0	25	-	-	-				
F	P1	1130	560	-	-	2.0[h]	0.41	0.0008	0.017	0.05
	P2	2880	15 500	-	-	0.2				

[a] Sedimentation rates are based on OSL dating (where a depth of 0 cm = time 0 years). Mean levee heights are calculated from topographic surveys of each (palaeo)channel belt (see Fig. 2A for location of surveys).

[b] Mid-point of the OSL age, expressed in years prior to the measurement date of A.D. 2015 (see Table 2).

[c] Samples T1-8 and T10-12 were collected during fieldwork in 2008, hence the recorded depth is from 2008, whilst the measured age is years prior to 2015. Sedimentation rate calculations (depth/age) for these samples have been adjusted by subtracting seven years from the calculated age.

[d] Levee heights calculated from highest point on the levee to lowest point on the floodplain surface within 150 m of the channel.

[e] Ratio of downstream gradient to cross-floodplain gradient.

[f] Denotes the time-averaged mean sedimentation rate to the surface where two OSL samples were taken from the same profile in vertical sequence (see Fig. 6).

[g] Sedimentation rate between two samples in the profile indicative of the sedimentation rates during waning fluvial activity along the reach.

[h] This alluvial ridge sedimentation rate along the Pienaars palaeochannel F is likely an underestimation. Sedimentation on the ridge is unlikely to occur post-abandonment, so the assumption that the surface equals zero years may not be strictly valid. Nonetheless, it provides a likely minimum sedimentation rate for that particular location.

5. Interpretation

The late Holocene avulsion history on the lower Tshwane River is well constrained by aerial photograph interpretation and OSL dating and demonstrates that at least three avulsions have occurred over the last ~650 years at ca. 630-530 a (palaeochannel B), ca. 550 a

(palaeochannel C), and ca. 120-75 a (palaeochannel E) in the ~4-km-long study reach. Palaeochannel infill rates during the waning phases of channel activity range from 6.1 to 23.5 mm a^{-1}, bracketing the levee sedimentation rate of 11.5 mm a^{-1} adjacent to the modern channel, while time-averaged sedimentation rates for palaeochannels that incorporate the waning and post-abandonment phases are slower, ranging from ~3.0 to ~7.4 mm a^{-1}.

Along with field observations, these results provide insights into the mechanisms of avulsion in this semiarid setting. Particularly noteworthy is the marked contrast between the moderate to high sinuosity reaches of most palaeochannels and some very low sinuosity reaches of the modern channel, especially the reach formed during the 1950-1972 avulsion (Figs. 1C, 2A-B, 3B-D). The OSL results (sample T5) show that until ~110 years ago, active transport of medium-coarse sand was occurring along the highly sinuous (~2.7), leveed, palaeochannel belt D (Figs. 3A, 5). Development of this high sinuosity channel would have reduced the reach-scale gradient, thereby contributing to a reduction in sediment transport capacity and inducing deposition.

The OSL dating in this reach (sample T4) confirms that the channel was still transporting some fine sand ~75 years ago (ca. A.D. 1940; Tables 2 and 3; Fig. 5), but infilling was clearly underway. This in-channel sedimentation would have decreased channel cross-sectional area, which is likely to have caused an increasing proportion of floodwaters to be diverted overbank, some of which would have flowed down the cross-floodplain gradient provided by the levees and into the backswamp that formerly existed on the western floodplain margin. This set of processes moved the reach closer to an avulsion threshold. During the falling stage of floods, these overbank floodwaters would have drained from the backswamp back into the channel via a low point or a breach in the bank, forming a small

headcut sometime between A.D. 1950 and 1972 (see point ii in Fig. 3A). Observed modern headcuts in the early stages of formation are ~1 m tall and up to ~20 m long (Fig. 2C). During successive floods, this headcut would have retreated upvalley and cut a newer, straighter channel through the backswamp. Once this headward-eroding channel reconnected with the original channel, most flow and sediment would have been diverted down the new channel (channel E) and the original channel would have been abandoned to form palaeochannel D. The length of channel E indicates that the headcut retreated a total distance of 760 m, while the OSL ages show that levee sedimentation had started adjacent to the new channel by ~60 years ago (ca. A.D. 1955). This suggests that flow and sediment diversion was already occurring by this date and indicates that channel E may have formed very rapidly over a 5-10 year period (a headcut retreat rate of between ~76 and 152 m a^{-1}). Following final abandonment, palaeochannel D would have infilled more rapidly, particularly at its upstream and downstream ends where inundation by overbank flows or backflooding from the newly-formed channel would occur more frequently, as is indicated by the loss of definition on aerial photographs (Fig. 3B).

The mechanism of incisional avulsion appears to be the dominant avulsion style along the floodplain wetlands of the lower Tshwane River. Crevasse splays are not developed anywhere along the study reach, suggesting that progradational avulsions are not important in this setting; and there is no evidence for reoccupational avulsions. The dominance of incisional avulsion explains the marked variations in channel sinuosity along the modern Tshwane River and can be used to conceptualise the sequence of changes that have driven repeated avulsions in this setting (Fig. 7). A newly-formed channel in a floodplain topographic low such as a backswamp is initially relatively straight, but over time bank

erosion leads to a net increase in sinuosity while overbank sedimentation builds levees. Increasing sinuosity leads to a reduction in local channel slope and a greater propensity for in-channel sedimentation, gradually priming the reach for avulsion and abandonment (Fig. 7). Once avulsion has taken place, sinuosity again begins to increase along the newly-formed, straight channel. In essence, the lower Tshwane River consists of a series of linked reaches of different sinuosity that broadly reflect the differing periods of time since each of those reaches formed by avulsion. Evidence from the most recent avulsion shows that the avulsion process was initiated and completed within ~50 to 100 years, a timescale that can be tentatively applied to the other, older avulsions in the study reach (Fig. 7).

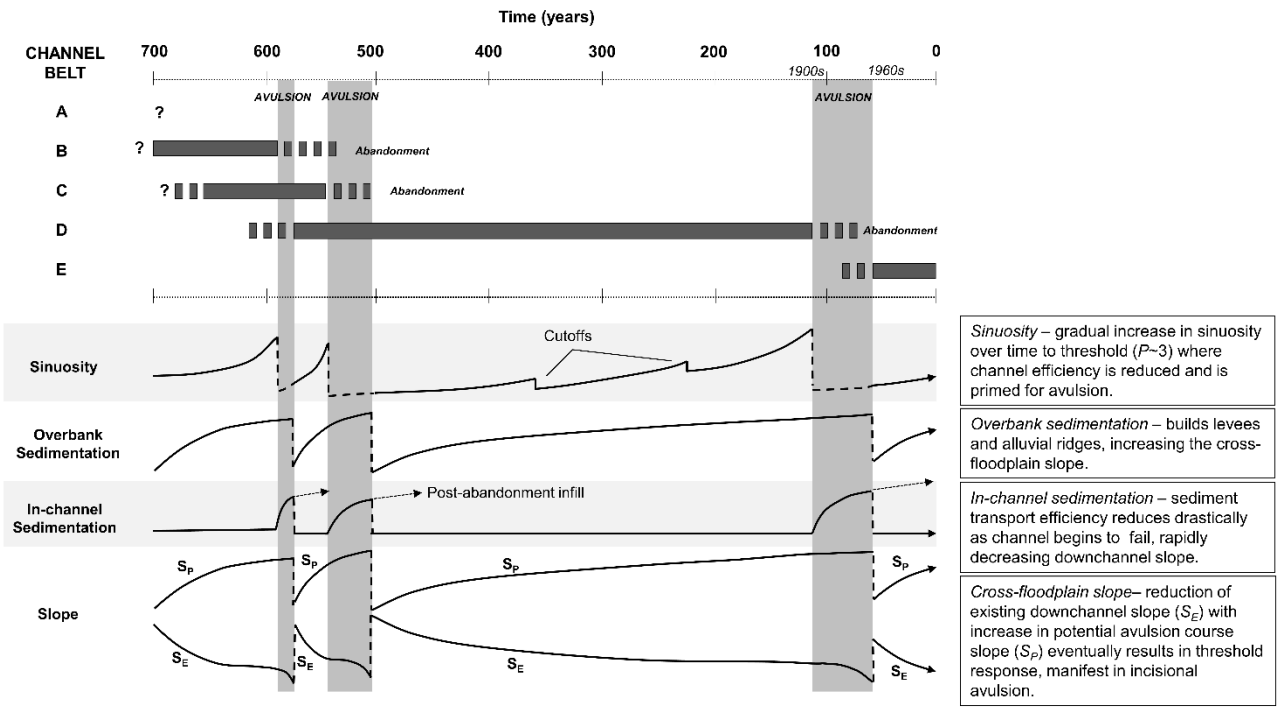

Fig. 7. Diagrammatic representation of the sequence of avulsions on the lower Tshwane River over the last 600-700 years. Solid horizontal bars represent channel activity and the discontinuous ends represent the initial and terminal stages of channel activity. The lower half of the diagram is a schematic illustration of the threshold responses driving avulsion.

These observations and interpretations can be used to predict the most likely locations of future avulsions in the study reach. In particular, some of the highly sinuous reaches upstream of the newly formed reach of the modern channel (channel E) appear to be primed for avulsion, including the reach containing a recent cutoff (point iii in Fig. 3C) as well as other reaches farther south. In one of these reaches, field observations show that a small headcut has begun to retreat upvalley through a backswamp located between the levee of the modern channel and the hillslope (Fig. 2C; for location, see Fig. 3D), and this may provide the next avulsion pathway. High resolution monitoring of this headcut could help to constrain further the characteristic rates of headcut retreat and the timescales of avulsion in this setting.

6. Discussion

The results and interpretations presented above document and explain the late Holocene avulsion history of the Tshwane-Pienaars floodplain wetlands but also provide original field data that advance our knowledge of the timescales, mechanisms, and controls of avulsions more generally.

6.1. Avulsion frequency, style, and sedimentation rates

Despite considerable research on river avulsions (e.g., Slingerland and Smith, 2004; Stouthamer and Berendsen, 2007), relatively few well-constrained field data sets exist that relate avulsion frequency, avulsion style, and sedimentation rates. There are older palaeochannels on the lower Tshwane floodplain that have not been addressed in this study (e.g., the undated palaeochannel belt A; Figs. 2A, 5), but the results show that at least three

avulsions have occurred over the last ~650 years, which equates to ~4.6 avulsions ka^{-1}. This high avulsion frequency appears to be associated with relatively rapid sedimentation, with vertical sedimentation rates >10 mm a^{-1} occurring within and adjacent to the channels, such as on the levee adjacent to the newly formed reach of the modern channel. Although the levee sedimentation rate (11.5 mm a^{-1}) presented for channel belt E is based on a single OSL age, it is the most relevant rate for comparing to avulsion frequency because levee and broader alluvial ridge development is a key determinant of the increase in cross-valley gradient that promotes erosion of a new headcutting channel. The palaeochannel infill sedimentation rates are less relevant as drivers of avulsion because these reflect either sedimentation that occurs after the initiation of the headcuts that ultimately lead to avulsion or include the sedimentation that occurs during the post-abandonment phase. Nonetheless, the sedimentation rates for the waning phases of channel activity (6.1 to 23.5 mm a^{-1}) bracket the levee sedimentation rate determined for channel belt E and support the interpretation that aggradation is occurring across parts of the lower Tshwane floodplain wetlands.

These results for avulsion frequency and sedimentation rate on the lower Tshwane River add another data point to the data set presented by Tooth et al. (2007; Fig. 8) and lend further support to the common assumption of a positive relationship between the two variables (e.g., Tornqvist and Bridge, 2002; Slingerland and Smith, 2004). Direct comparisons of avulsion frequency and sedimentation rate between different rivers are not straightforward, with published studies having used different sampling strategies and geochronological techniques, and employed various analytical approaches to calculate the relevant variables over different timescales (for details, see Fig. 8 caption and the original

studies). Some of the data points on Fig. 8 are for anabranching rivers (e.g., Rhine-Meuse, upper Columbia, lower Saskatchewan), which complicates the comparisons with avulsion frequencies along single-thread rivers (e.g., Klip River, Tshwane River) because, all other factors being equal, avulsion frequencies should be higher where there is a greater total length of channels per kilometer of valley. Nonetheless, although various caveats surround each of the data points, the results presented here are sufficient to highlight the distinctive plotting position of the lower Tshwane River, at least during the late Holocene.

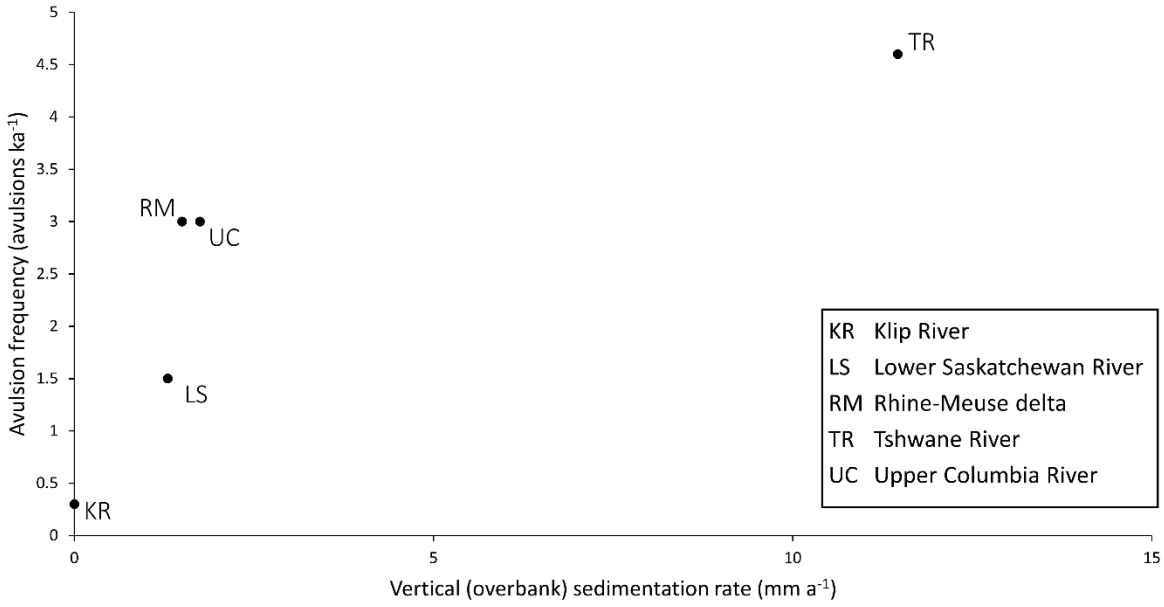

Fig. 8. Graph illustrating the relationship between sedimentation rate and avulsion frequency, adapted from Tooth et al. (2007). Data for the lower Saskatchewan River, Rhine-Meuse delta, and upper Columbia River are taken from the compilation in Makaske et al. (2002, their Table 5). The sedimentation rate for the lower Saskatchewan River is the average for peat and organic-rich sediments derived using radiocarbon dating and may underestimate long-term sedimentation rate (Morozova and Smith, 2000). The sedimentation rate for the upper Columbia River is an average of floodplain and levee sedimentation rates derived using radiocarbon dating (Makaske et al., 2002). The sedimentation rate for the Rhine-Meuse delta represents the rate before compaction (Stouthamer and Berendsen, 2001; Makaske et al., 2002). The long-term (>1 ka) sedimentation

rate for the Klip River is assumed to be zero as the channel remains grounded on bedrock, and so it is inferred that there is no net, long-term vertical aggradation (Tooth et al., 2007).

Previous work has suggested possible relationships between avulsion style and sedimentation rate, highlighting that incisional avulsions tend to be associated with slowly aggrading rivers and progradational avulsions with more rapidly aggrading rivers (Makaske, 2001; Slingerland and Smith, 2004; Tooth et al., 2007; Table 1). Importantly, however, the findings from the lower Tshwane River demonstrate that incisional avulsions can be the dominant mechanism even in relatively rapidly aggrading rivers. In stark contrast to other moderately to rapidly aggrading rivers with frequent avulsions (Smith et al., 1989; Makaske et al., 2002), the absence of crevasse splays shows that progradational avulsions are not a feature of the lower Tshwane River, and there is no evidence for reoccupational avulsions. Broadly speaking, incisional avulsions and vertical sedimentation rates do not appear to be closely coupled; incisional avulsions can occur across a range of rivers with widely differing sedimentation rates from effectively zero or barely above zero (e.g., Knighton and Nanson, 1993; Gibling et al., 1998; Tooth et al., 2007, 2009) to relatively rapid (>5 mm a^{-1}; e.g., Ralph et al., 2011, 2016; this study).

6.2 Relative importance of intrinsic and extrinsic controls of avulsion

Outstanding questions remain about the relative importance of intrinsic (e.g., flow-sediment dynamics) and extrinsic (e.g., tectonic, climatic) controls of avulsion. In tectonically stable settings, changing hydroclimates potentially can influence avulsion dynamics, particularly through their influence on flow magnitude and frequency (e.g., Grenfell et al., 2014). Some studies have highlighted the fact that avulsion frequencies have been higher during wetter

past climates (e.g., Stouthamer and Berendsen, 2000, 2001), while other studies have been more equivocal, finding no clear evidence of changes in avulsion frequency related to changes in climate. For instance, by comparing an ~30 ka avulsion record for the upper Klip River, South Africa, with a range of late Quaternary palaeoclimatic proxy records, Tooth et al. (2007) found no correlation between avulsion frequency and regional climatic changes, arguing that incisional avulsions on this river have not been extrinsically forced but instead have occurred intrinsically as a natural outcome of meander-belt development.

Although the OSL-constrained avulsion record for the lower Tshwane River covers a much shorter timescale than the record for the Klip River (Tooth et al., 2007), similar cause-and-effect reasoning can be applied. Palaeoenvironmental proxy records derived from Namibian hyrax middens, a nearby crater lake core (Tswaing Crater), and a cave speleothem (Makapansgat Cold Air Cave) show that in the last ~650 years there has been some regional climatic variability, particularly around the time of the Little Ice Age (LIA; Partridge et al., 1997; Tyson, 1999; Lee-Thorp et al., 2001; Chase et al., 2010, 2012; Burrough and Thomas, 2013). However, there is no apparent correlation between the three late Holocene avulsions of the Tshwane River and regional climate variability, with the avulsions occurring during slightly cooler and drier conditions ~600-500 years ago and during warmer, moister modern conditions in the past ~100 years. Hence, like the Klip River, avulsion on the lower Tshwane appears to be an intrinsic process related to meander-belt development. In particular, a marked increase in sinuosity along a developing meander belt is associated with a decrease in sediment transport capacity and channel cross-sectional area, both of which contribute to the development of incisional avulsions (Fig. 7).

While the correlations with regional palaeoclimatic records indicate no causal link between changing hydroclimates and the timing of particular incisional avulsion events, a comparison of the avulsion records for the Klip and Tshwane rivers nevertheless provides a tentative indication that the overall hydroclimatic setting may exert a subtle influence on the propensity for avulsion. In the reaches that are dominated by avulsion, both rivers are very similar in terms of planform and cross-sectional morphology, riparian vegetation assemblages, sediment characteristics, and the range of floodplain features present (e.g., oxbows, palaeochannels, and backswamps). Yet despite these similarities, aerial photograph analyses and OSL dating reveals very different timeframes of fluvial change. The Klip River exhibits very slow lateral migration rates (<0.16 m a^{-1}), with only three cutoffs having occurred in the ~28-km-long study reach since 1954 (Tooth et al., 2009). Avulsion frequency is low (~0.3 avulsions ka^{-1} since ~15 ka), with the last natural avulsion having occurred ~1000 years ago, although an anthropogenically forced avulsion is currently ongoing (Tooth et al., 2007, 2009). These infrequent avulsions have occurred under conditions of no net long-term vertical sedimentation, for despite local levees and alluvial ridges, channel beds essentially remain grounded on bedrock (Rodnight et al., 2005; Marren et al., 2006; Tooth et al., 2007, 2009; Keen-Zebert et al., 2013). By contrast, the Tshwane River exhibits faster lateral migration rates, with 14 cutoffs occurring in the ~4-km-long study reach since 1950, and avulsion frequency is much higher (~4.6 avulsions ka^{-1}). Levees and alluvial ridges are more prominent features, with vertical sedimentation rates in and around channels locally >10 mm a^{-1}. Consequently, channel beds are decoupled from underlying bedrock, with the thickness of floodplain alluvium exceeding 7 m (Fig. 5).

A tentative proposition that remains to be tested by further research is that these contrasting avulsion behaviours are related to differences in regional climate (Larkin et al., in press), as reflected in a differing aridity index for each system, which is defined by mean annual precipitation divided by mean annual potential evaporation (United Nations Environment Program, 1992; Working for Wetlands, 2008; Gauteng Department of Agriculture and Rural Development, 2011). The Klip River floodplain wetlands are located in a subhumid setting with an aridity index of 0.42. Discharge, stream power, and channel size increase slightly downstream, and sediment throughput is maintained (Marren et al., 2006; Tooth et al., 2009). Owing to the slow lateral migration rates, channel reaches take centuries to thousands of years to develop moderate or high sinuosities (>1.5), and so incisional avulsions occur only infrequently. In contrast, the Tshwane River floodplain wetlands are located in a semiarid setting with an aridity index of 0.33. Discharge, stream power, and channel size all decrease downstream (Table A.2), and sediment throughput is not maintained (Larkin et al., in press). Consequently, there is a greater tendency for long-term vertical sediment accumulation within and near the channel. Lateral migration occurs more rapidly, with channel reaches taking only decades to centuries to develop moderate or high sinuosities, which primes the river for more frequent incisional avulsions (Fig. 7).

Tentatively, these findings suggest that there may be a systematic, climatically influenced transition or a series of thresholds between subhumid, slowly adjusting (Klip-type) systems and semiarid, more rapidly adjusting (Tshwane-type) systems. Additional chronologically constrained avulsion data sets from rivers in differing hydroclimatic settings are required to test this proposition and define these relationships further. If the proposition is broadly supported, however, this may provide valuable insight into possible changes to channel

dynamics in floodplain wetlands, which is particularly important in view of the projections for drier and more variable future climates in many drylands globally (Cook et al., 2014; Pachauri et al., 2014; Pascale et al., 2016).

7. Conclusion

River avulsion is a complex process that is influenced by a range of regional and site-specific factors, and the relationships between sedimentation rate, frequency, and styles of avulsion remain to be fully clarified. Chronologically controlled, field-based data sets are essential for defining these relationships and for providing input to computational models of avulsion. In this study of the lower Tshwane River, analysis of historical aerial photographs and OSL dating reveal that three avulsions have occurred over the last 650 years. Local sedimentation rates >10 mm a^{-1} occur within and adjacent to the channel, leading to levee and alluvial ridge development. The increase in cross-floodplain gradient primes certain reaches for avulsion by promoting erosion of a new channel on the lower-lying floodplain.

The findings from the lower Tshwane River support the hypothesis that there is a positive relationship between sedimentation rate and avulsion frequency and show that incisional avulsions can occur along rivers undergoing relatively rapid net aggradation. In this setting, the lack of correspondence between regional climatic changes and the timing of specific avulsion events suggests that avulsions have not been extrinsically forced but instead occur intrinsically as an integral part of meander-belt development. Nevertheless, comparison with the avulsion chronology for another South African river system tentatively suggests that the overall hydroclimatic setting may exert a subtle influence on the propensity for avulsion, with incisional avulsions likely to occur more frequently in semiarid settings than in subhumid settings. Future research should aim to identify and investigate other avulsive

rivers across a range of hydroclimatic settings so that additional chronological data sets can be developed to test this proposition and further define these relationships.

Acknowledgements

This research was funded by a British Society for Geomorphology Postgraduate Research Grant (Larkin), a National Geographic Young Explorers Grant (Larkin, Ralph, Tooth, and McCarthy, No. 9670-15), Macquarie University postgraduate research funds (Larkin), and the National Research Foundation (McCarthy). This material is based upon work supported by the National Science Foundation under Grant No. 0754345 (Keen-Zebert). Additional fieldwork costs were supported by discretionary research funds (Ralph) and the Aberystwyth University Research Fund (Tooth), and funding from the Climate Change Consortium of Wales (Tooth) contributed to OSL analyses. We thank Hollie Wynne for processing and measuring the OSL samples and Michael Grenfell for providing historical aerial photos of the Tshwane River. We also thank Ian Rutherford, Matt Rowberry, three anonymous reviewers, and Co-Editor-in-Chief Dick Marston for helpful comments that substantially improved the original submitted manuscript.

References

Aitken, M.J., 1998. An introduction to optical dating: the dating of Quaternary sediments by the use of photon-stimulated luminescence: Oxford University Press.

Aslan, A., Blum, M.D., 1999. Contrasting styles of Holocene avulsion, Texas Gulf coastal plain, USA. In Smith ND and Rogers J (Eds), Fluvial Sedimentology VI, International Association of Sedimentologists, Special Publication No. 28. Oxford: Blackwell Scientific Publications, pp.193-209.

Aslan, A., Autin, W.J., Blum, M.D., 2005. Causes of river avulsion: insights from the late Holocene avulsion history of the Mississippi River, USA. Journal of Sedimentary Research 75: 650-664. DOI: 10.2110/jsr.2005.053

Assine, M.L., 2005. River avulsions on the Taquari megafan, Pantanal wetland, Brazil. Geomorphology 70: 357-371. DOI: 10.1016/j.geomorph.2005.02.013

Bjerklie, D.M., 2007. Estimating the bankfull velocity and discharge for rivers using remotely sensed river morphology information. Journal of Hydrology 341 : 144-155. DOI:10.1016/j.jhydrol.2007.04.011

Bøtter-Jensen, L., Andersen, C.E., Duller, G.A.T., Murray, A.S., 2003. Developments in radiation, stimulation and observation facilities in luminescence measurements. Radiation Measurements 37: 535-541. DOI: 10.1016/S1350-4487(03)00020-9

Bridge, J.S. Leeder, M.R., 1979. A simulation model of alluvial stratigraphy. Sedimentology 26: 617-644. DOI: 10.1111/j.1365-3091.1979.tb00935.x

Brizga, S.O. Finlayson, B.L., 1990. Channel avulsion and river metamorphosis: The case of the Thomson River, Victoria, Australia. Earth Surface Processes and Landforms 15: 391-404. DOI: 10.1002/esp.3290150503

Bryant, M., Falk, P., Paola, C., 1995. Experimental study of avulsion frequency and rate of deposition. Geology 23: 365-368. DOI: 10.1130/0091-7613(1995)023<0365:ESOAFA> 2.3.CO;2

Burrough, S.L. Thomas, D.S.G., 2013. Central southern Africa at the time of the African Humid Period: A new analysis of Holocene palaeoenvironmental and palaeoclimate data. Quaternary Science Reviews, 80: 29-46. DOI: 10.1016/j.quascirev.2013.08.001

Chase, B.M., Meadows, M.E., Carr, A.S., Reimer, P.J., 2010. Evidence for progressive Holocene aridification in southern Africa recorded in Namibian hyrax middens: Implications for African Monsoon dynamics and the 'African Humid Period'. Quaternary Research, 74: 36-45. DOI: 10.1016/j.yqres.2010.04.006

Chase, B.M., Scott, L., Meadows, M.E., Gil-Romera, G., Boom, A., Carr, A.S., Reimer, P.J., Truc, L., Valsecchi, V., Quick, L.J., 2012. Rock hyrax middens: A palaeoenvironmental archive for southern African drylands. Quaternary Science Reviews, 56: 107-125. DOI: 10.1016/j.quascirev.2012.08.018

Cook, B.I., Smerdon, J.E., Seager, R., Coats, S., 2014. Global warming and 21st century drying. Climate Dynamics, 43: 2607-2627. DOI: 10.1007/s00382-014-2075-y

Department of Water Affairs Hydrological Services, 2015. Hydrological Services - Surface Water (Data, Dams, Floods and Flows), https://www.dwa.gov.za/Hydrology/, retrieved: 22/05/15

Donselaar, M.E., Cuevas Gozalo, M.C., Moyano, S., 2013. Avulsion processes at the terminus of low-gradient semi-arid fluvial systems: Lessons from the Rio Colorado, Altiplano endorheic basin, Bolivia. Sedimentary Geology 283: 1-14. DOI: 10.1016/j.sedgeo.2012.10.007

Duller, G.A.T., 2003. Distinguishing quartz and feldspar in single grain luminescence measurements. Radiation Measurements 37: 161-165. DOI: 10.1016/S1350-4487(02)00170-1

Duller, G.A.T., 2004. Luminescence dating of Quaternary sediments: recent advances. Journal of Quaternary Science 19: 183-192. DOI: 10.1002/jqs.809

Duller, G.A.T., 2015. The Analyst software package for luminescence data: overview and recent improvements. Ancient TL 33: 35-42.

Ellery, W., Dahlberg, A., Strydom, R., Neal, M., Jackson, J., 2003. Diversion of water flow from a floodplain wetland stream: an analysis of geomorphological setting and hydrological and ecological consequences. Journal of Environmental Management. 68: 51-71. DOI: 10.1016/S0301-4797(03)00002-1

Fuchs, M.C., Kreutzer, S., Burow, C., Dietze, M., Fischer, M., Schmidt, C., Fuchs, M., 2015. Data processing in luminescence dating analysis: An exemplary workflow using the R package 'Luminescence'. Quaternary International 362: 8-13. DOI: 10.1016/j.quaint.2014.06.034

Galbraith, R.F., Roberts, R.G., Laslett, G., Yoshida, H., Olley, J.M., 1999. Optical dating of single and multiple grains of quartz from Jinmium rock shelter, northern Australia: part i, experimental design and statistical models. Archaeometry 41: 339-364. DOI: 10.1111/j.1475-4754.1999.tb00987.x

Gauteng Department of Agriculture and Rural Development, (G.D.A.R.D.), 2011. Gauteng State of the Environment Report 2011. Gauteng Provincial Government.

Gibling, M.R., Nanson, G.C., Maroulis, J.C., 1998. Anastomosing river sedimentation in the Channel Country of central Australia. Sedimentology 45: 595-619. DOI: 10.1046/j.1365-3091.1998.00163.x

Grenfell, S.E., Grenfell, M.C., Rowntree, K.M., Ellery, W.N., 2014. Fluvial connectivity and climate: A comparison of channel pattern and process in two climatically contrasting fluvial sedimentary systems in South Africa. Geomorphology 205: 142-154. DOI: 10.1016/j.geomorph.2012.05.010

Hajek, E.A., Edmonds, D.A., 2014. Is river avulsion style controlled by floodplain morphodynamics? Geology 42: 199-202. DOI: 10.1130/G35045.1

Hajek, E.A., Wolinsky, M., 2012. Simplified process modeling of river avulsion and alluvial architecture: Connecting models and field data. Sedimentary Geology 257-260: 1-30. DOI: 10.1016/j.sedgeo.2011.09.005

Jacobs, Z., Duller, G.A.T., Wintle, A.G. 2006. Interpretation of single grain D_e distributions and calculation of D_e. Radiation Measurements 41: 264-277. DOI: 10.1016/j.radmeas.2005.07.027

Jain, V., Sinha, R., 2004., Fluvial dynamics of an anabranching river system in Himalayan foreland basin, Baghmati River, north Bihar plains, India. Geomorphology 60: 147-170. DOI: 10.1016/j.geomorph.2003.07.008

Jerolmack, D.J., Mohrig, D., 2007. Conditions for branching in depositional rivers. Geology 35: 463-466. DOI: 10.1130/G23308A.1

Jones, L., Schumm, S., 1999. Causes of avulsion: an overview. In Smith ND and Rogers J (Eds), Fluvial Sedimentology VI, International Association of Sedimentologists, Special Publication No. 28. Oxford: Blackwell Scientific Publications, pp. 171-178.

Judd, D.A., Rutherfurd, I.D., Tilleard, J.W., Keller, R.J., 2007. A case study of the processes displacing flow from the anabranching Ovens River, Victoria, Australia. Earth Surface Processes and Landforms 32: 2120-2132. DOI: 10.1002/esp.1516

Keen-Zebert, A., Tooth, S., Rodnight, H., Duller, G., Roberts, H., Grenfell, M., 2013. Late Quaternary floodplain reworking and the preservation of alluvial sedimentary archives in unconfined and confined river valleys in the eastern interior of South Africa. Geomorphology 185: 54-66. DOI: 10.1016/j.geomorph.2012.12.004

Knighton, D., Nanson, G., 1993. Anastomosis and the continuum of channel pattern. Earth Surface Processes and Landforms 18: 613-625. DOI: 10.1002/esp.3290180705

Larkin, Z.T., Ralph, T.J., Tooth, S., McCarthy, T., in press. The interplay between extrinsic and intrinsic controls in determining floodplain wetland characteristics in the South African drylands. Earth Surface Processes and Landforms. DOI: 10.1002/esp.4075

Lee-Thorp, J.A., Holmgren, K., Linge, H., Moberg, A., Partridge, T.C., Stevenson, C., Tyson, P.D., 2001. Rapid climate shifts in the southern African interior throughout the mid to late Holocene. Geophysical Research Letters, 28: 4507-4510. DOI: 10.1029/2000GL012728

Li, J., Bristow, C.S., 2015. Crevasse splay morphodynamics in a dryland river terminus: Río Colorado in Salar de Uyuni Bolivia. Quaternary International, 377: 71-82. DOI:10.1016/j.quaint.2014.11.066

Li, J., Donselaar, M.E., Hosseini Aria, S.E., Koenders, R., Oyen, A.M., 2014. Landsat imagery-based visualization of the geomorphological development at the terminus of a dryland river system. Quaternary International, 352: 100-110. DOI:10.1016/j.quaint.2014.06.041

Mackey, S.D. Bridge, J.S., 1995. Three-dimensional model of alluvial stratigraphy: theory and application. Journal of Sedimentary Research 65, 7-31.

Macklin, M.G., Lewin, J., 2015. The rivers of civilization. Quaternary Science Reviews, 114: 228-244. DOI:10.1016/j.quascirev.2015.02.004

Makaske, B., 2001. Anastomosing rivers: A review of their classification, origin and sedimentary products. Earth Science Reviews 53: 149-196. DOI: 10.1016/S0012-8252(00)00038-6

Makaske, B., Maathuis, B.H.P., Padovani, C.R., Stolker, C., Mosselman, E., Jongman, R.H.G., 2012. Upstream and downstream controls of recent avulsions on the Taquari megafan, Pantanal, south-western Brazil. Earth Surface Processes and Landforms 37: 1313-1326. DOI: 10.1002/esp.3278

Makaske, B., Smith, D.G., Berendsen, H.J., 2002. Avulsions, channel evolution and floodplain sedimentation rates of the anastomosing upper Columbia River, British Columbia, Canada. Sedimentology 49: 1049-1071. DOI: 10.1046/j.1365-3091.2002.00489.x

Marren, P.M., McCarthy, T.S., Tooth, S., Brandt, D., Stacey, G.G., Leong, A., Spottiswoode, B., 2006. A comparison of mud- and sand-dominated meanders in a downstream coarsening reach of the mixed bedrock-alluvial Klip River, eastern Free State, South Africa. Sedimentary Geology, 190: 213-226. DOI: 10.1016/j.sedgeo.2006.05.014

McCarthy, T., Ellery, W., Stanistreet, I., 1992. Avulsion mechanisms on the Okavango fan, Botswana: the control of a fluvial system by vegetation. Sedimentology 39: 779-795. DOI: 10.1111/j.1365-3091.1992.tb02153.x

Morozova, G.S., 2005. A review of Holocene avulsions of the Tigris and Euphrates Rivers and possible effects on the evolution of civilizations in lower Mesopotamia. Geoarchaeology 20: 401-423. DOI:10.1002/gea.20057

Morozova, G.S., Smith, N.D., 2000. Holocene avulsion styles and sedimentation patterns of the Saskatchewan River, Cumberland Marshes, Canada. Sedimentary Geology 130: 81-105. DOI: 10.1016/S0037-0738(99)00106-2

Pachauri, R.K., Allen, M., Barros, V., Broome, J., Cramer, W., Christ, R., Church, J., Clarke, L., Dahe, Q., Dasgupta, P., 2014. Climate Change 2014: Synthesis Report. Contribution of Working Groups I, II and III to the Fifth Assessment Report of the Intergovernmental Panel on Climate Change.

Partridge, T., Demenocal, P., Lorentz, S., Paiker, M., Vogel, J., 1997. Orbital forcing of climate over South Africa: a 200,000-year rainfall record from the Pretoria Saltpan. Quaternary Science Reviews 16: 1125-1133. DOI: 10.1016/S0277-3791(97)00005-X

Pascale, S., Lucarini, V., Feng, X., Porporato, A., ul Hasson, S., 2016. Projected changes of rainfall seasonality and dry spells in a high greenhouse gas emissions scenario. Climate Dynamics, 46: 1331-1350. DOI:10.1007/s00382-015-2648-4

Phillips, J.D., 2009. Avulsion regimes in southeast Texas rivers. Earth Surface Processes and Landforms 34: 75-87. DOI:10.1002/esp

Phillips, J.D., 2011. Universal and local controls of avulsions in southeast Texas Rivers. Geomorphology, 130(1-2): 17-28. DOI: 10.1016/j.geomorph.2010.10.001

Phillips, J.D., 2012. Log-jams and avulsions in the San Antonio River Delta, Texas. Earth Surface Processes and Landforms, 37: 936-950. DOI:10.1002/esp.3209

Polvi, L.E., Wohl, E., 2013. Biotic drivers of stream planform implications for understanding the past and restoring the future. BioScience 63: 439-452. DOI: 10.1525/bio.2013.63.6.6

Prescott, J.R., Hutton, J.T., 1994. Cosmic ray contributions to dose rates for luminescence and ESR dating: large depths and long-term time variations. Radiation Measurements 23: 497-500. DOI: 10.1016/1350-4487(94)90086-8

Ralph, T.J., Hesse, P.P., 2010. Downstream hydrogeomorphic changes along the Macquarie River, southeastern Australia, leading to channel breakdown and floodplain wetlands. Geomorphology 118: 48-64. DOI: 10.1016/j.geomorph.2009.12.007

Ralph, T.J., Hesse, P., Kobayashi, T., 2016. Wandering wetlands: spatial patterns of historical channel and floodplain change in the Ramsar-listed Macquarie Marshes, Australia. Marine and Freshwater Research 67: 782-802. DOI: 10.1071/MF14251

Ralph, T.J., Kobayashi, T., García, A., Hesse, P.P., Yonge, D., Bleakley, N., Ingleton, T., 2011. Paleoecological responses to avulsion and floodplain evolution in a semiarid Australian freshwater wetland. Australian Journal of Earth Sciences 58: 75-91. DOI: 10.1080/08120099.2010.534818

Rodnight. H., Duller, G., Tooth, S., Wintle, A., 2005. Optical dating of a scroll-bar sequence on the Klip River, South Africa, to derive the lateral migration rate of a meander bend. The Holocene 15: 802-811. DOI: 10.1191/0959683605hl854ra

Rodnight, H., Duller, G.A., Wintle, A.G., Tooth, S., 2006. Assessing the reproducibility and accuracy of optical dating of fluvial deposits. Quaternary Geochronology 1: 109-120. DOI: 10.1016/j.quageo.2006.05.017

Schumm, S.A., Erskine, W.D., Tilleard, J.W., 1996. Morphology, hydrology, and evolution of the anastomosing Ovens and King Rivers, Victoria, Australia, Bulletin of the Geological Society of America 108: 1212-1224. DOI: 10.1130/0016-7606(1996)108<1212:MHAEOT>2.3.CO;2

Slingerland, R., Smith, N.D., 1998. Necessary conditions for a meandering-river avulsion. Geology 26: 435-438. DOI: 10.1130/0091-7613(1998)026<0435:NCFAMR>2.3.CO;2

Slingerland, R., Smith, N.D., 2004. River avulsions and their deposits. Annual Review of Earth & Planetary Sciences 32: 257-285. DOI: 10.1146/annurev.earth.32.101802.120201

Smith, D.G., Pearce, C.M., 2002. Ice jam-caused fluvial gullies and scour holes on northern river flood plains. Geomorphology 42: 85-95. DOI:10.1016/S0169-555X(01)00076-9

Smith, N.D., Cross, T.A., Dufficy, J.P., Clough, S.R., 1989. Anatomy of an avulsion. Sedimentology 36: 1-23. DOI: 10.1111/j.1365-3091.1989.tb00817.x

Smith, N.D., McCarthy, T.S., Ellery, W., Merry, C.L., Rüther, H., 1997. Avulsion and anastomosis in the panhandle region of the Okavango Fan, Botswana. Geomorphology 20: 49-65. DOI: 10.1016/S0169-555X(96)00051-7

Stouthamer, E., Berendsen, H.J.A., 2000. Factors controling the Holocene avulsion history of the Rhine-Meuse Delta (The Netherlands). Journal of Sedimentary Research, 70: 1051-1064. DOI: 10.1306/033000701051

Stouthamer, E., Berendsen, H.J.A., 2001. Avulsion frequency, avulsion duration, and interavulsion period of Holocene channel belts in the Rhine-Meuse Delta, The Netherlands. Journal of Sedimentary Research, 71: 589-598. DOI: 10.1306/112100710589

Stouthamer, E., Berendsen, H.J.A., 2007. Avulsion: The relative roles of autogenic and allogenic processes. Sedimentary Geology 198: 309-325. DOI: 10.1016/j.sedgeo.2007.01.017

Tooth, S., 1999. Floodouts in central Australia. In Miller AJ and Gupta A (Eds), Varieties of Fluvial Form. John Wiley and Sons Ltd., Chichester, United Kingdom, pp.219-247.

Tooth, S., 2005. Splay formation along the lower reaches of ephemeral rivers on the northern plains of arid central Australia. Journal of Sedimentary Research, 75: 636-649. DOI: 10.1002/9781444304213.ch8

Tooth, S., Rodnight, H., Duller, G.A.T., McCarthy, T.S., Marren, P.M., Brandt, D., 2007. Chronology and controls of avulsion along a mixed bedrock-alluvial river. Geological Society of America Bulletin 119: 452-461. DOI: 10.1130/B26032.1

Tooth, S., Rodnight, H., McCarthy, T.S., Duller, G.A.T., Grundling, A.T., 2009. Late Quaternary dynamics of a South African floodplain wetland and the implications for assessing recent human impacts. Geomorphology 106: 278-291. DOI: 10.1016/j.geomorph.2008.11.009

Törnqvist, T.E., Bridge, J.S., 2002. Spatial variation of overbank aggradation rate and its influence on avulsion frequency. Sedimentology 49: 891-905. DOI: 10.1046/j.1365-3091.2002.00478.x

Tyson, P., 1999. Late-Quaternary and Holocene palaeoclimates of Southern Africa; a synthesis. South African Journal of Geology 102: 335-349.

United Nations Environment Program (UNEP), 1992. World Atlas of Desertification. Edward Arnold, London: 15-45.

Wentworth, C.K., 1922. A scale of grade and class terms for clastic sediments. The Journal of Geology: 377-392.

Wintle, A.G., Murray, A.S., 2006. A review of quartz optically stimulated luminescence characteristics and their relevance in single-aliquot regeneration dating protocols. Radiation Measurements 41: 369-391. DOI: 10.1016/j.radmeas.2005.11.001

Working for Wetlands, 2008. Borakalalo A23J – Wetland Rehabilitation Plan, Report no. L02218/180208/1, South African National Biodiversity Institute.

Appendices

Table A.1. Summary of downstream trends in channel characteristics, discharge and stream power along the Tshwane River (after Larkin et al., in press).

Reach	Average sinuosity [a]	Average floodplain width (± SD; km) [b]	Average channel width (± SD; m) [c]	Bankfull discharge ($m^3 s^{-1}$) [d]	Unit stream power ($W m^{-2}$) [d]	Bed material
Confined headwaters	1.00 - 1.20	0.05 ± 0.09	20.7 ± 6.5	> 40	> 30	Bedrock, sand and gravel
Partly confined middle reaches	1.20 – 1.70	0.31 ± 0.29	19.3 ± 4.0	~20-40	~ 15-20	Mud, sand and minor gravel – partly alluvial
Unconfined lower reaches (floodplain wetlands)	1.50 – 2.70	1.13 ± 0.28	10.9 ± 1.5	< 15	< 10	Mud, sand and minor gravel – fully alluvial

[a] Sinuosity measured along 1 km reaches of the channel (channel distance/straight line distance).
[b] Floodplain width measured every kilometre downstream. Boundary between floodplain and valley hillslope estimated using topographic data derived from a 30 m DEM of the region and distinct vegetation zonation patterns (hillslope vegetation vs. floodplain vegetation).
[c] Bankfull channel width measured every 1 km downstream, generally focusing on straighter sections to avoid results being skewed by local increases in channel width at meander bends.
[d] Following the method of Bjerklie (2007), discharge and stream power were modelled for the rivers using remotely sensed channel morphology data.

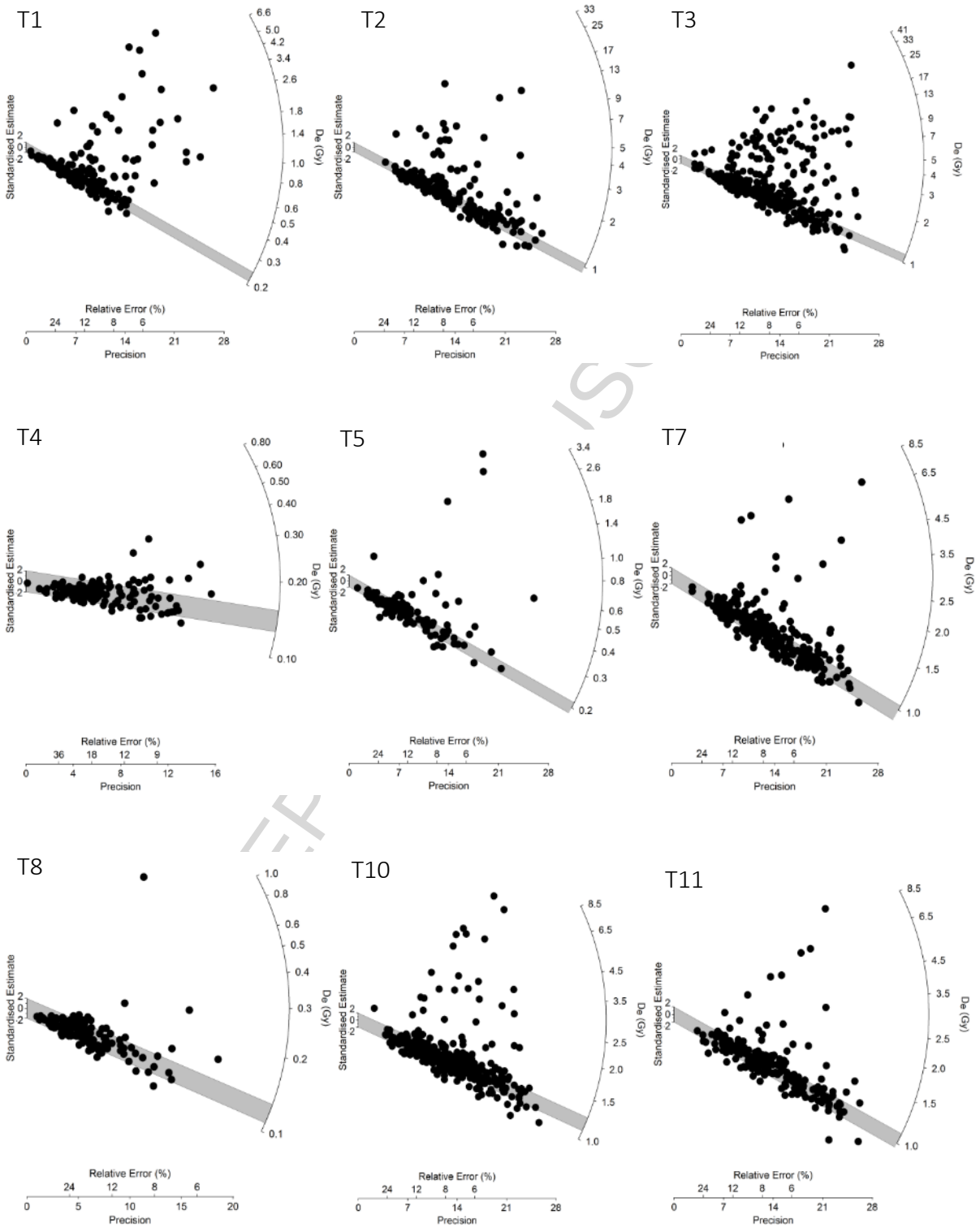

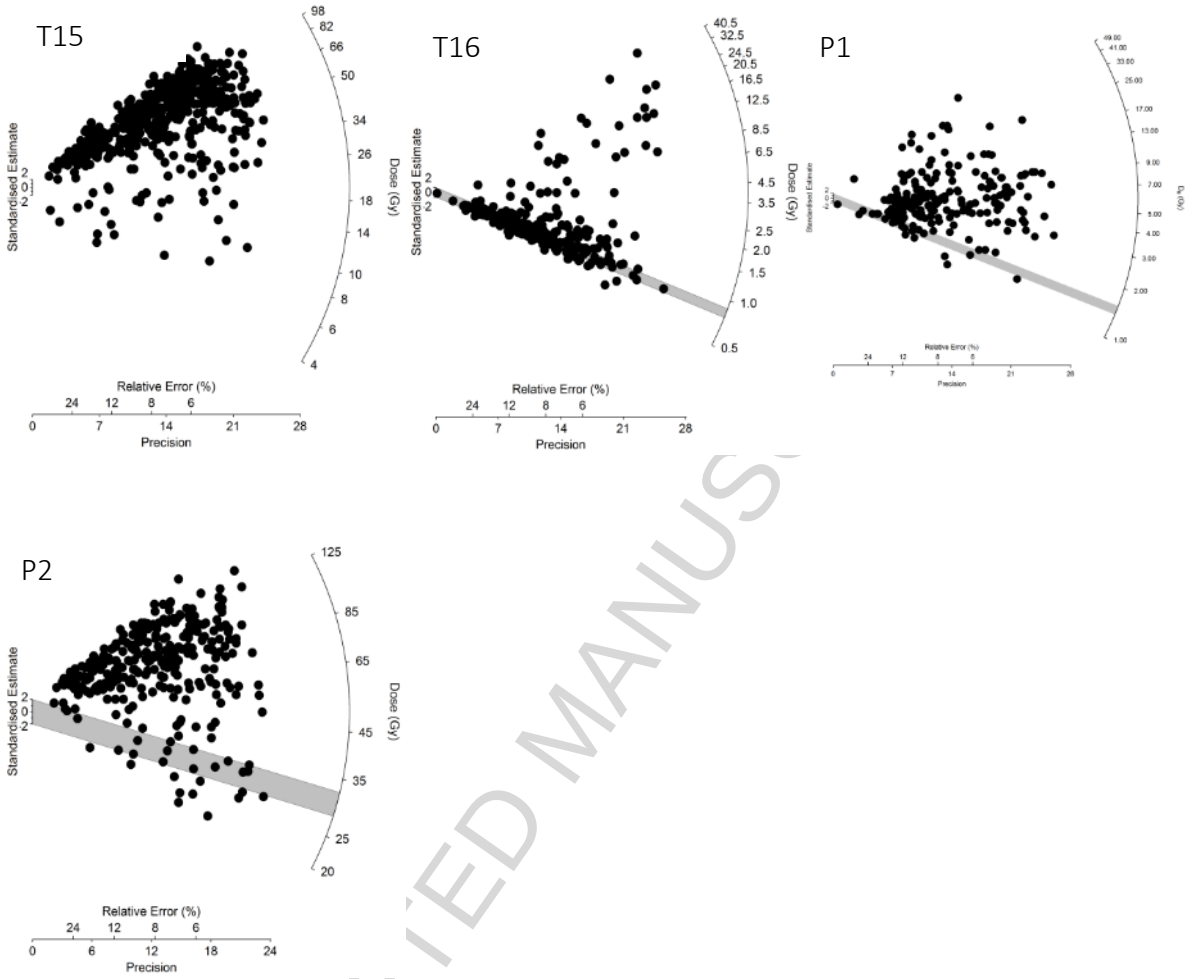

Figure A.1 Radial plots of equivalent dose (D_e) values from individual grains of quartz for the Tshwane River and Pienaars River OSL samples. The full code for samples is Aber219/TSW or Aber219/PC but for illustrative purposes and brevity, codes have been simplified to a prefix 'T' or 'P'. The grey shaded bar represents the minimum D_e given by the minimum age model (MAM). Samples T12 and T14 are too young to display in a log scale radial plot due to some negative D_e values. Note the unusual D_e distribution of sample T15. The minimum age model could not provide a minimum D_e estimate with such a distribution, and as such an age estimate has not been given for T15.

Table A.2 OSL dosimetry data for the Tshwane River samples

Sample[a]	Depth (m)	Water content (%)[b]	Grain size (µm)	Beta Dose (Gy ka^{-1})[c]	Gamma Dose (Gy ka^{-1})[d]	Cosmic Dose (Gy ka^{-1})[e]	Total Dose Rate (Gy ka^{-1})
T1	1.05 ± 0.10	25 ± 5	125-250	0.93 ± 0.06	0.84 ± 0.08	0.19 ± 0.01	1.96 ± 0.10
T2	1.60 ± 0.10	25 ± 5	180-212	0.92 ± 0.05	0.76 ± 0.07	0.18 ± 0.01	1.86 ± 0.09
T3	2.15 ± 0.10	25 ± 5	150-212	0.79 ± 0.05	0.78 ± 0.07	0.17 ± 0.01	1.74 ± 0.08
T4	0.38 ± 0.08	25 ± 5	180-212	0.86 ± 0.05	0.72 ± 0.06	0.23 ± 0.02	1.81 ± 0.08
T5	0.85 ± 0.05	25 ± 5	150-212	0.91 ± 0.05	0.81 ± 0.07	0.20 ± 0.01	1.91 ± 0.09
T7	1.68 ± 0.10	25 ± 5	180-212	0.68 ± 0.04	0.69 ± 0.06	0.18 ± 0.01	1.54 ± 0.08
T8	0.55 ± 0.05	15 ± 5	150-180	1.10 ± 0.07	0.96 ± 0.08	0.22 ± 0.01	2.27 ± 0.11
T10	1.48 ± 0.08	25 ± 5	180-212	1.00 ± 0.06	0.89 ± 0.08	0.18 ± 0.01	2.07 ± 0.10
T11	1.95 ± 0.10	25 ± 5	180-212	0.83 ± 0.05	0.76 ± 0.07	0.17 ± 0.01	1.76 ± 0.08
T12	0.53 ± 0.08	25 ± 5	180-212	0.68 ± 0.04	0.58 ± 0.05	0.22 ± 0.01	1.47 ± 0.06
T14	0.00 ± 0.05	25 ± 5	150-212	0.43 ± 0.03	0.42 ±0.04	0.31 ± 0.01	1.16 ± 0.05
T15	1.81 ± 0.10	25 ± 5	150-212	0.84 ± 0.05	0.74 ± 0.05	0.17 ± 0.01	1.76 ± 0.08
T16	2.10 ± 0.10	25 ± 5	180-212	0.71 ± 0.04	0.66 ± 0.05	0.17 ± 0.01	1.54 ± 0.07
P1	1.13 ± 0.13	15 ± 5	180-212	0.95 ± 0.09	0.96 ± 0.09	0.19 ± 0.01	2.10 ± 0.11
P2	2.88 ± 0.13	15 ± 5	180-212	0.87 ± 0.05	0.78 ± 0.06	0.15 ± 0.01	1.80 ± 0.08

[a] The full code for samples is Aber219/TSW or Aber219/PC but for illustrative purposes and brevity have been simplified to a prefix 'T' or 'P'.

[b] Water content used to calculate the total dose rate. Water content was measured and kept constant for palaeochannel and oxbow samples at 25 ± 5 %, and at 15 ± 5 % for levee samples, which dry out more readily and regularly than samples in the base of infilling channels.

[c] Beta dose rate determined by beta counter measurements of dried and milled material taken from the ends of the sample tubes.

[d] Gamma dose rate determined by thick source alpha counting of dried and milled material taken from the ends of the sample tubes.

[e] The cosmic ray contribution was estimated from the data given by Prescott and Hutton (1994), taking into account altitude, geomagnetic latitude and thickness of sediment overburden.